

Photodeformable Azobenzene-Containing Liquid Crystal Polymers and Soft Actuators

Xinlei Pang, Jiu-an Lv, Chongyu Zhu, Lang Qin, and Yanlei Yu*

Photodeformable liquid crystal polymers (LCPs) that adapt their shapes in response to light have aroused a dramatic growth of interest in the past decades, since light as a stimulus enables the remote control and diverse deformations of materials. This review focuses on the growing research on photodeformable LCPs, including their basic actuation mechanisms, the various deformation modes, the newly designed molecular structures, and the improvement of processing techniques. Special attention is devoted to the novel molecular structures of LCPs, which allow for easy processing and alignment. The soft actuators with various deformation modes such as bending, twisting, and rolling in response to light are also covered with the emphasis on their photo-induced bionic functions. Potential applications in energy harvesting, self-cleaning surfaces, sensors, and photo-controlled microfluidics are further illustrated. The existing challenges and future directions are discussed at the end of this review.

a reversible and alignment-dependent shape-change behavior of liquid crystals (LCs).^[7,14–16] The first example of photo-induced deformation of the crosslinked liquid crystal elastomer (CLCP), realized a 20% spontaneous contraction, igniting a new competition in this field.^[17] Beyond pursuing CLCPs with better photodeformability for simple contraction/expansion, scientists have also put great efforts in the development of the 3D motion of these CLCPs to obtain more complex functions, including bending,^[18–20] twisting,^[21] oscillating,^[22–25] etc., for practical applications such as soft actuators.

In the past decades, researchers devoted much effort to the innovation of materials with newly designed molecular structures. Recent advances in LCPs, such as the introduction of post-crosslinkable

1. Introduction


Stimuli-responsive polymers, whose actuators actively undergo a predetermined change in the geometry when excited by a stimulus, opening a door to the development of advanced polymers for remote actuation. Among them, photoresponsive polymers with photomechanical conversion ability are a rising star on the horizon of smart materials owing to the advantages of light for remote, instantaneous, localized, and precise control.^[1–10] The pioneer work of light-controlled deformation of photoresponsive polymers was done in the last century, i.e., azobenzene-containing polymer in the amorphous state shrunk about 1% under illumination.^[11–13] Much effort was made to develop new photoresponsive polymers with better photodeformable performances subsequent to this work. Liquid crystal polymers (LCPs), especially the ordered ones, have demonstrated their potentials to dramatically increase the photodeformation extent and construct light-driven soft actuators because they possess fascinating features combining the entropic elasticity of polymeric elastomers and the ability to undergo

moieties, provide a facile way to prepare large-scale LCP films and fibers with different shapes, and present the advantage to control the properties of materials by simply changing the crosslinking agents. Introducing dynamic covalent bonds makes it possible to realign mesogens and reshape formed polymer networks. Furthermore, LCPs without chemical crosslinking networks have demonstrated improved processing performance compared with the traditional crosslinked systems.

The innovation in materials opens the way to a wide range of processing techniques, especially benefits for the fabrication of microstructures. The traditional one-step method is applicable for the preparation of LCP films using the LC cells to achieve different alignments (planar, homeotropic, splay, or twist) by proper modification of the alignment layers.^[1,26] Recently, researchers have developed some industrial compatible methods for the fabrication of microstructured LCP actuators, such as inkjet printing,^[20] replica molding,^[27] direct laser writing (DLW),^[28] microfluidics,^[29,30] etc. For instance, replica molding technique makes it possible to fabricate different patterned LCPs with high reproducibility over centimeter scale distances in a short time.

The innovative materials and processing techniques give to scientists a chance to get a step closer to actuators as found in nature. Complex natural systems that exist in biological life are the result of a long evolution. For instance, vine plants always ensure their own survival by virtue of other organisms. In order to seek out dependence, they must transform living spaces constantly to retain a place in fierce competitions in the woods, and thereby most of them have chosen a mode of spiral movement. Learning from the relationship between structures

X. Pang, Dr. J. Lv, Dr. C. Zhu, Dr. L. Qin, Prof. Y. Yu
Department of Materials Science & State Key Laboratory of Molecular Engineering of Polymers
Fudan University
220 Handan Road, Shanghai 200433, China
E-mail: ylyu@fudan.edu.cn

 The ORCID identification number(s) for the author(s) of this article can be found under <https://doi.org/10.1002/adma.201904224>.

DOI: 10.1002/adma.201904224

and functions of animals and plants, various bioinspired photodeformable LCP actuators, such as inching walker,^[31] artificial cilia,^[20] winding ribbons,^[21] artificial seedpots,^[32] artery-like tubes,^[30] etc., have been demonstrated over the decades.

Here, we provide a brief overview of the development as well as the cutting edge of photodeformable LCPs. The basic mechanisms of photodeformations are presented at the beginning, followed by an introduction of diverse LCP actuators. Especially, actuators with unique properties and functions inspired from nature are highlighted throughout the text. New types of LCPs such as post-crosslinked LCPs, dynamic crosslinked LCPs, and linear LCPs, coupled with improved processing performance and deformation ability, will provide new inspiration for the design and fabrication of soft actuators. In addition, the researches related to the preparation of LCP macro- and micro-actuators by using various fabrication methods have also been outlined. Within this framework, we provide an outlook for the development of photodeformable LCPs in the near future following the trend of material demands.

2. Mechanisms of Photodeformation

Light-driven deformation of LCPs is induced by the shape and orientation variation of LC molecules, which can be amplified into a macroscopic shape change of materials. To understand the essence of photoresponsive behaviors of LCPs, the basic mechanisms of photodeformation are first discussed in the following.

2.1. Photo-Induced Phase Transition

LCPs containing photoisomerizable molecular switches undergo phase transition by either photochemical or photothermal effects. Photochemical effects are generally based on the *trans-cis* isomerization of azobenzene mesogens (Figure 1a). With the accumulation of the *cis* isomer generated by photoisomerization, the LCP undergoes a phase transition from a LC phase to an isotropic state.^[33,34] The photothermal effect, on the other hand, is an effective mean to convert light into heat, which increases the system temperature above the LC-isotropic phase transition temperature and then disrupts the alignment direction of the mesogens. Photothermal effect occurs in the presence of photothermal agents such as azobenzene derivatives,^[35] metal nanoparticles,^[36] and organic or organometallic dyes^[37–39] (Figure 1c). These photothermal actuations have been well reviewed in other literatures.^[40–42] Despite the fact that the photothermal effect is always existed in azobenzene-based actuators, the photochemical phase transition of the LCP is typically designed for actuation. The detailed mechanism is shown below.

Due to the cooperative effect in LC molecules, the energy required to induce the alignment change of only 1 mol% of LC molecules in response to an external stimulus is enough to change the alignment of the whole system.^[1,2,34] When a photochromic molecule or moiety is introduced into the LC system, a phase transition is triggered isothermally by the photochemical reaction of photochromic molecules after light illumination.^[43] Over the last decades, diverse photochromic molecules have been developed, such as azobenzenes, diarylethenes, spiropyran,



Xinlei Pang is currently a Ph.D. student at the Department of Materials Science, Fudan University (China), where she received her M.S. degree in 2017 under the supervision of Prof. Y. L. Yu. She received her B.S. degree in the Department of Materials Science and Engineering at Donghua University (China) in 2015. Her research interests focus on the design and construction of liquid crystal polymers and soft actuators.



Jiu-an Lv received the M.S. degree in polymer physics and chemistry from Northwest University, China in 2008. During the following 3 years, he worked as a process engineer at the China Aerospace Science and Technology Corp. He earned his Ph.D. degree in material chemistry and physics in 2016 from Fudan University and continued his research in Fudan University as a postdoctoral research fellow. His research interests focus on the design of functional polymer materials and the exploration of their applications.



Yanlei Yu is a professor in the Department of Materials Science at Fudan University, China. She graduated in applied chemistry from Anhui University in 1993 and obtained her M.S. degree in polymer chemistry and physics from the University of Science and Technology of China in 1996. She gained her Ph.D. degree in environmental chemistry and engineering from Tokyo Institute of Technology and was promoted to full professor at Fudan University in 2004. Her research interests focus on the development of photodeformable smart materials and light-controllable interface materials with photosensitive polymers and liquid crystal polymers.

burgeoning hydrazones, etc.^[44,45] Azobenzene derivatives (usually simply referred to as “azobenzenes”) have remained by far the widely used photochromic molecules for converting light into mechanical deformation.^[15] Azobenzenes have two isomeric states: a rod-like *trans* configuration that stabilizes the

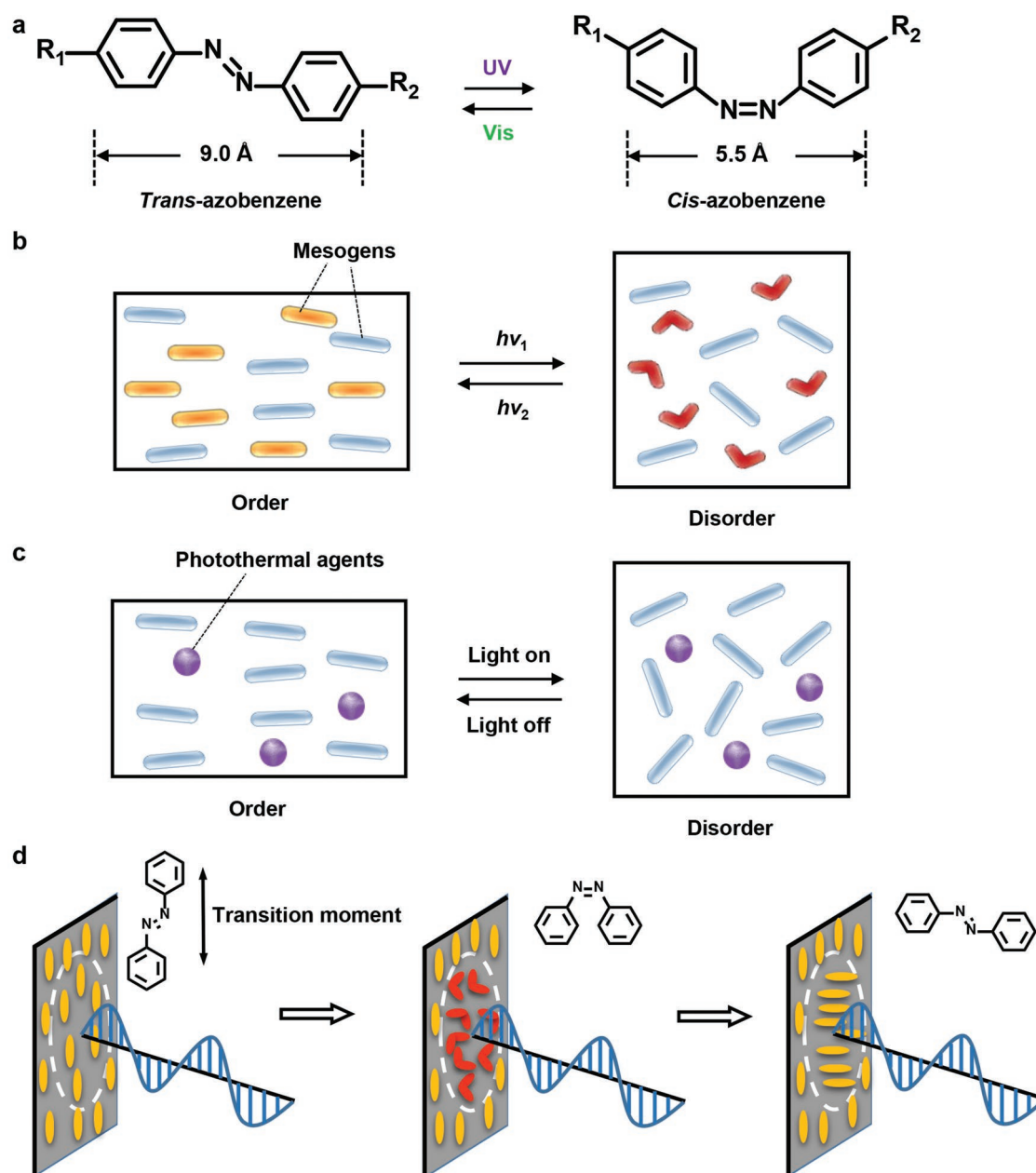


Figure 1. a) Reversible *trans*–*cis* photoisomerization of azobenzenes. b,c) Schematic representation of b) photo-induced and c) photothermal-induced order–disorder phase transition in LCPs. b,c) Reproduced with permission.^[87] Copyright 2019, Wiley-VCH. d) Photoreorientation of azobenzene-containing LCPs with linearly unpolarized light. Reproduced with permission.^[8] Copyright 2017, Acta Polymerica Sinica.

structure of LC phase, and a bent-shape *cis* isomer that tends to destabilize the LC phase (Figure 1b).^[46] The *trans*–*cis* isomerization of azobenzene is usually induced by UV light irradiation, which causes the conformational changes of the azobenzenes.^[47] Photochemical phase transition is reversible, thus a sample returns to the initial LC phase via the *cis*-to-*trans* isomerization of azobenzenes by thermal relaxation or visible-light irradiation.

The incorporation of azobenzene units into CLCPs provides the possibility of photo-induced deformation. Irradiation of an azobenzene-containing CLCP with UV light will disrupt the alignment order of LC molecules and induce a phase transition

from the ordered LC state to the isotropic phase, and eventually lead to a macroscopic anisotropic deformation of the entire crosslinked network. Such deformation of LC systems induced by phase transition is generally reversible and thus has unique deformation controllability.^[1–9,26,34,43,46,48–51]

2.2. Photoreorientation (the Weigert Effect)

A special photochemical property of azobenzenes is photo-induced orientation upon polarized light irradiation, which is

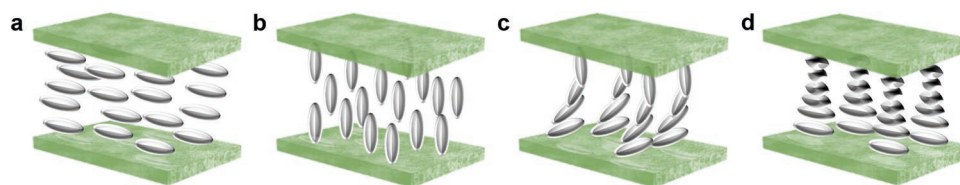


Figure 2. Schematic illustrations of different LC molecular orientations. Uniaxial alignments: a) planar and b) homeotropic. Besides uniaxial alignments, the LCs can be ordered in c) splayed and d) twisted configurations.

known as the Weigert effect.^[5,52] As shown in Figure 1d, when transition moments (long axis) of *trans*-azobenzene molecules are parallel to the polarization direction of linearly polarized light, azobenzenes absorb energy into an excited state, and then undergo the *trans*–*cis* isomerization. Azobenzenes with transition moments perpendicular to the polarization direction do not absorb light and, no isomerization occurs. After repeated *trans*–*cis*–*trans* isomerization cycles, transition moments of *trans*-azobenzenes will be perpendicular to the polarization direction of light and they become insensitive to the incident light, therefore, no more isomerization happens.

Except for the aforementioned photo-induced reorientation process, there is another photo-induced orientation process called out-of-plane orientation.^[53,54] When illuminating azobenzene-containing LCPs with unpolarized light or circularly polarized light, only one direction (the propagation direction) is perpendicular to the electric field vector of light. Thus, azobenzenes are prone to align with the molecular axis along the propagation direction of the incident light. By changing the direction of the incident light, the azobenzenes are manipulated three dimensionally.

3. Photodeformation

3.1. Contraction and Expansion

In 1975, deGennes et al. first proposed that the deformation of monodomain nematic CLCP strongly relies on the order degree of LC molecules.^[55,56] They then reported an intriguing theoretical study on the probability of employing CLCPs as artificial muscles.^[56] They proposed that well-aligned CLCPs exhibited reversible thermomechanical response induced by thermal-induced phase transition. If incorporating azobenzenes into CLCPs, the photochemical phase transition will be realized, and then triggers the deformation of CLCPs by light. The group of Finkelmann preceded in the synthesis of monodomain azobenzene-containing CLCPs with polysiloxanes as the main chains.^[17] They theoretically predicted that such CLCPs could generate shape changes between 10% and 400% upon illumination, and experimentally achieved the light-actuated contraction by up to 20% when fueled with UV light after about 1 h. This work manifests the significant reversible mechanical deformation generated by CLCPs with a stimulation of light, which has pioneered the research of photodeformable LCP materials.

Subsequent synthetic efforts by other academics have quickly followed, mainly aiming for materials with faster response and larger deformation.^[18,43,57] Keller and co-workers reported the synthesis of side-on acrylate-based CLCPs containing

azobenzene moieties in the side chains by photo-polymerization with a near-infrared photoinitiator.^[57] Side-chain polymers in which mesogens are attached via a flexible spacer are distinguished between end-on (the mesogen is fixed at its end) and side-on (the mesogen is fixed in the middle).^[26] Comparing these two mesogen architectures, the side-on systems have a stronger chain anisotropy due to the stronger coupling between mesogens and backbone. Upon exposure to UV light at 70 °C for about 1 min, the thin film exhibited a fast photo-induced contraction of up to 18%. This work plays a crucial role in the enhancement of response speed of photoactive CLCPs.

3.2. Topographical Deformation

The alignment is not an intrinsic property of the LC but is controlled by employing external fields (electric, magnetic, light, etc.) or alignment layers. In the monomeric state, various molecular configurations are established as shown in Figure 2. Typically, two main alignments are obtained: uniaxial planar (Figure 2a) or homeotropic (Figure 2b), meaning that the molecules either lay parallel or stand perpendicular to the substrate. Alignment gradients over the thickness of the sample are also realized such as the splay (rotation in the *xz*-plane, Figure 2c) or the twist (rotation in the *xy*-plane, Figure 2d) alignments. LC alignments ordered in the *z*-direction that perpendicular to the substrate produce diverse, often complex, topological deformations of LCPs. The topological deformation is the local deviations of a surface switching from a perfectly flat state to a predetermined deformed state by an external trigger, which leads to many new applications.

In the LC system, the order degree of rod-like LC molecules is defined with the vector n and the order parameter S , $S = \frac{1}{2}(3\cos^2\theta - 1)$, here θ is the deviation angle between LC molecules and the vector n ($0 < \theta < \pi/2$). The decrease of the order degree of LCP films induced by light allows for the increase of the value of θ . Thus, the sample contracts along the orientation direction of LCs ($n_{||}$) (contraction rate is λ , $\lambda < 1$), while expands perpendicularly to the direction of the alignment of LCs (n_{\perp}) (expansion rate is $\lambda^{-\nu}$, ν is the Poisson's ratio of materials). LCP films that deform into 3D shapes are prepared using continuous, circular director alignment patterns.^[58] These continuous alignment patterns are based on declinations of LCs, i.e., the topological defects of LCs. This sort of declination is defined by the alignment of LC mesogens centers on the declinational singularity, and the strength m of the declination is defined as the number of cycles of LC mesogens rotating 360° around the declinational singularity (Figure 3a).^[58,59] The

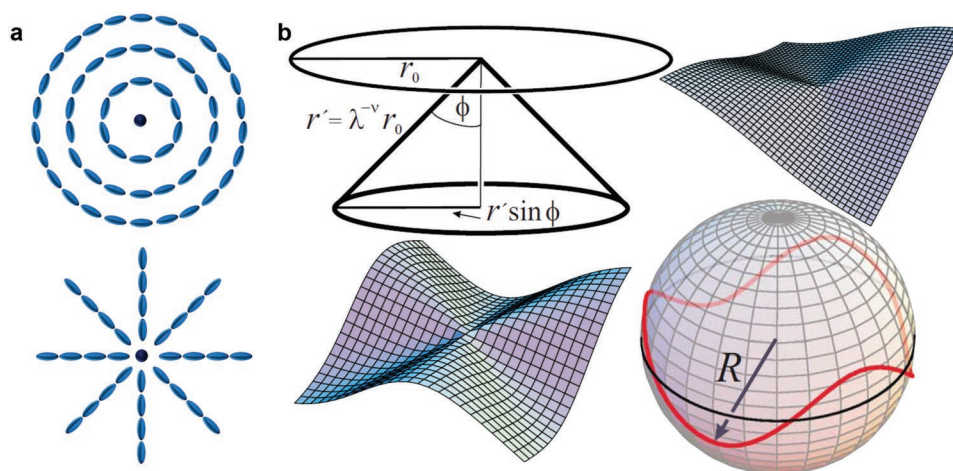


Figure 3. a) Examples of $m = +1$ azimuthal disclination (top) and $m = +1$ radial disclination (bottom). b) Shape deformation of films with an $m = +1$ disclination pattern upon heating. A film with an azimuthal pattern will contract along the radius and expand along the circumference to form a cone with a base radius $r' \sin \phi$, where ϕ is the cone opening angle. A film with a radial pattern will form an anticone shape with a buckled circumference. Reproduced with permission.^[61] Copyright 2011, The Royal Society.

value of m is positive when the rotation direction of LC mesogens coincides with that of the LC vector, conversely, is negative. A related theory has predicted the topological deformation of LCP films with a $+1$ declinational alignment pattern in a thermal-responsive system.^[58,60,61] In the case of a disk-shaped LCP film with an azimuthal alignment, its circumference was $C = 2\pi r$ (r is the radius of sample). Upon heating, LC mesogens changed from ordered state to disordered state, leading to a new radius $r' = \lambda^{-\nu} r$ and a new circumference $C' = \lambda C$ of the sample, where $0 < \lambda < 1$ and $\nu > 0$. That is, the radius increased and the circumference decreased after deformation. In order to accommodate this shape alteration, the sample was prone to deform into a “cone” shape (Figure 3b). Additionally, when a disk-shaped LCP film adopted a radial alignment, its radius and circumference changed to $r' = \lambda r$ and $C' = \lambda^{-\nu} C$, respectively. After the deformation, the radius of sample decreased and its circumference increased. The sample generated an “anticone” shape with a buckled circumference to adapt the dimensional changes. With strains increasing, the number of buckles increased, leading to a more crumpled anticone.

Photoalignment is proven to be an attractive method for patterning complex and diverse alignments into LCPs and thus yielding more complex actuations. Broer et al. fabricated a series of patterned LC cells by photoalignment technology.^[62] When molten acrylate LC precursors were injected into the cell, LCs spontaneously formed a variety of patterned alignments by means of the anchoring effect which was generated on patterned alignment layers, such as azimuthal, spiral, and radial patterns, and then these alignments were fixed by light curing. A reduction of the LC order induced by the photothermal effect was translated to a contraction behavior of sample along the preferred orientation of LCs. Thanks to patterned alignments, the CLCP films generated complex deformation such as cone and saddle shapes (Figure 4a). This work provides key momentum for the investigation of complex topological deformation of LCPs.

Also using the photoalignment technique, White et al. patterned topological defects into photoresponsive azobenzene-functionalized CLCPs and demonstrated diverse light-induced

topographical transformations of initially flat films with defects ranging from $-5/2$ to $+5/2$ (Figure 4b).^[63] Later on, they reported photo-induced deformation of complex topographical features with elastic sheets made from main-chain azobenzene-containing CLCPs (Figure 4c).^[64] Different from the previous work, the CLCPs used in this work were synthesized by the reaction between LC monomer mixtures and an amine via aza-Michael addition. Photoalignment technique was used to spatially program the local orientation of the nematic director. Upon irradiation with 365 nm UV light, the CLCP film with a $+1$ azimuthal defect in the center generated the conical deformation due to the decrease in nematic order induced by the *trans-cis* isomerization of azobenzenes. Then the formed conical domes returned to the flat state by irradiation with 532 nm visible light. Superior to the thermal-induced shape morphing of CLCPs, the geometry and actuation strain of elastic sheet in this work are remotely controlled in a precise manner.

Topographic textures on the surface of coating materials consist of gradual or steep concave or convex steps may vary from a macroscopic level of millimeters that have been just discussed to micrometers or even nanometers.^[65] Control of the surface topology in the micrometer range by active switching between a flat state to a preprogrammed corrugated state by light is of interest for a wide range of applications.^[66] Until now, various photoresponsive dynamic surface topographies based on azobenzene-functionalized CLCPs were presented. Particularly, the group of Broer has made intensive studies in this area. They prepared a patterned film containing planar chiral-nematic next to homeotropic areas by using a patterned indium tin oxide electrode glass cell (Figure 5a).^[67] Photoresponsiveness was enabled by the incorporation of a dimethacrylate azobenzene monomer, which was copolymerized with a chiral diacrylate monomer to induce the chiral nematic phase and other mono- or diacrylate LC monomers. By applying an electric field, the initial planar helicoidal molecular alignment was locally converted to the homeotropic orientation. Then, this dual alignment was fixed by the photo-polymerization step. Upon UV irradiation, these two types of molecular alignments

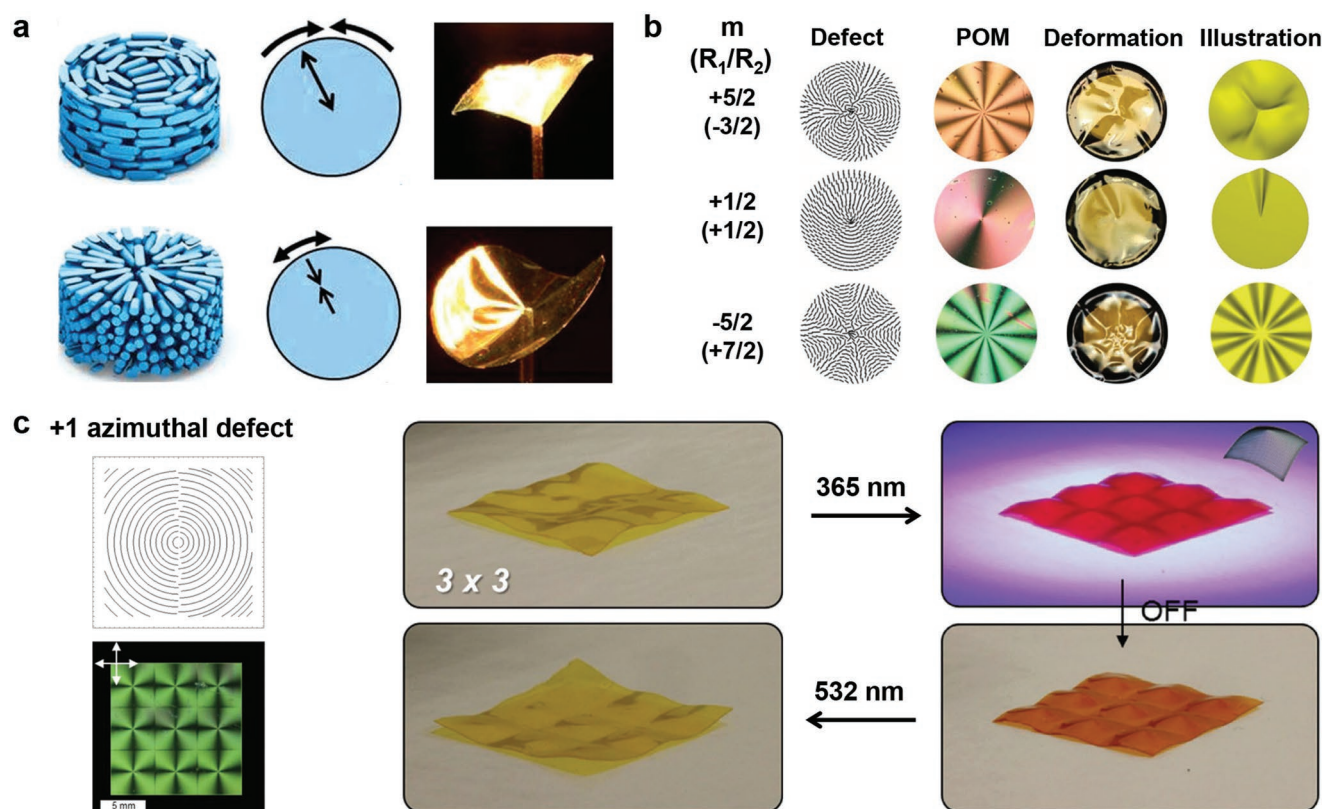


Figure 4. a) Actuation of films with azimuthal (top) and radial (bottom) alignments upon heating with an IR lamp. The arrows along the radius and the azimuth indicate the direction of deformation. Reproduced with permission.^[62] Copyright 2012, Wiley-VCH. b) Summary of the director field, polarized optical microscopy image (1 cm diameter), photomechanical response of film (1.2 cm diameter), and illustration of photomechanical response for azo-CLCP films subsumed with $+5/2$, $+1/2$, and $-5/2$ topological defects when subjected to unpolarized 445 nm light. The defect strength (m) and ratio of polarization rotation to sample rotation (R_1/R_2) are labeled for each row. Reproduced with permission.^[63] Copyright 2013, Wiley-VCH. c) An azobenzene-containing CLCP film with a 3×3 array of +1 azimuthal defects. Upon irradiation with 365 nm light, nine conical domes emerge from the film. The cones are metastable after removal of the UV light before being returned to the flat state by irradiation with 532 nm light. Reproduced with permission.^[64] Copyright 2016, Wiley-VCH.

exhibited opposite photomechanical response. In the homeotropic area, the reduction of molecular order induced by *trans-cis* isomerization of zenbenzenes resulted in expansion in the lateral direction and contraction perpendicular to the surface. For planar chiral-nematic area, it expanded perpendicular to the plane of film when the order parameter was reduced and showed zero or even negative expansion within the plane of film (Figure 5b). This suggested that for patterned surfaces in small scale the density decrease/volume increase was assisted by the order parameter reduction.^[66,68] The combination of two effects generated a large photomechanical deformation: a modulation amplitude close to 20% of the initial film thickness.

Although the effects demonstrated in the aforementioned work are striking, the fabrication of these patterned films is complicated and requires space-modulated electrical fields to produce localized homeotropic alignments. Broer and co-workers reported a worm-like fingerprint configuration by a self-assembling procedure to avoid lithographic patterning and the additional electric field (Figure 5c).^[69] Unlike the foregoing work with the helix axes in the planar area were normal to the substrate, the helix axes here rotated 90° by modification of the substrate surface. It is worth highlighting that the self-assembling method makes it possible to minimize the lateral

protrusion dimensions down to micrometer sizes or smaller simply by changing the concentration of chiral monomers. Upon UV light irradiation, azobenzenes underwent *trans-cis* isomerization and decreased the order parameter of the polymer network. The monomeric segments in the helices parallel to the surface tended to expand and formed protrusions, while the segments perpendicular to the surface contracted and generated wells (Figure 5d). As a result, the fingerprint textures showed an in-depth modulation up to 24% of the initial film thickness.

Although in the fingerprints work authors have eliminated the complex lithographic process to align the molecules, much efforts are still required to balance the two distinct forces between the chiral force and the anchoring force from the substrate that tend to rotate molecules in different directions. This phenomenon sets limits to the coating thickness that should be on the order of half the periodicity of the molecular helix in order to obtain stable fingerprint textures.^[66,70] Broer et al. further developed a simple and effective method to make the preparation of photoresponsive coatings easier based on polydomain LCs.^[70] In polydomain LCs, the molecules were aligned differently only within the domain regions but the domains with various alignments were randomly distributed with respect to each other (Figure 5e). Upon exposure to UV

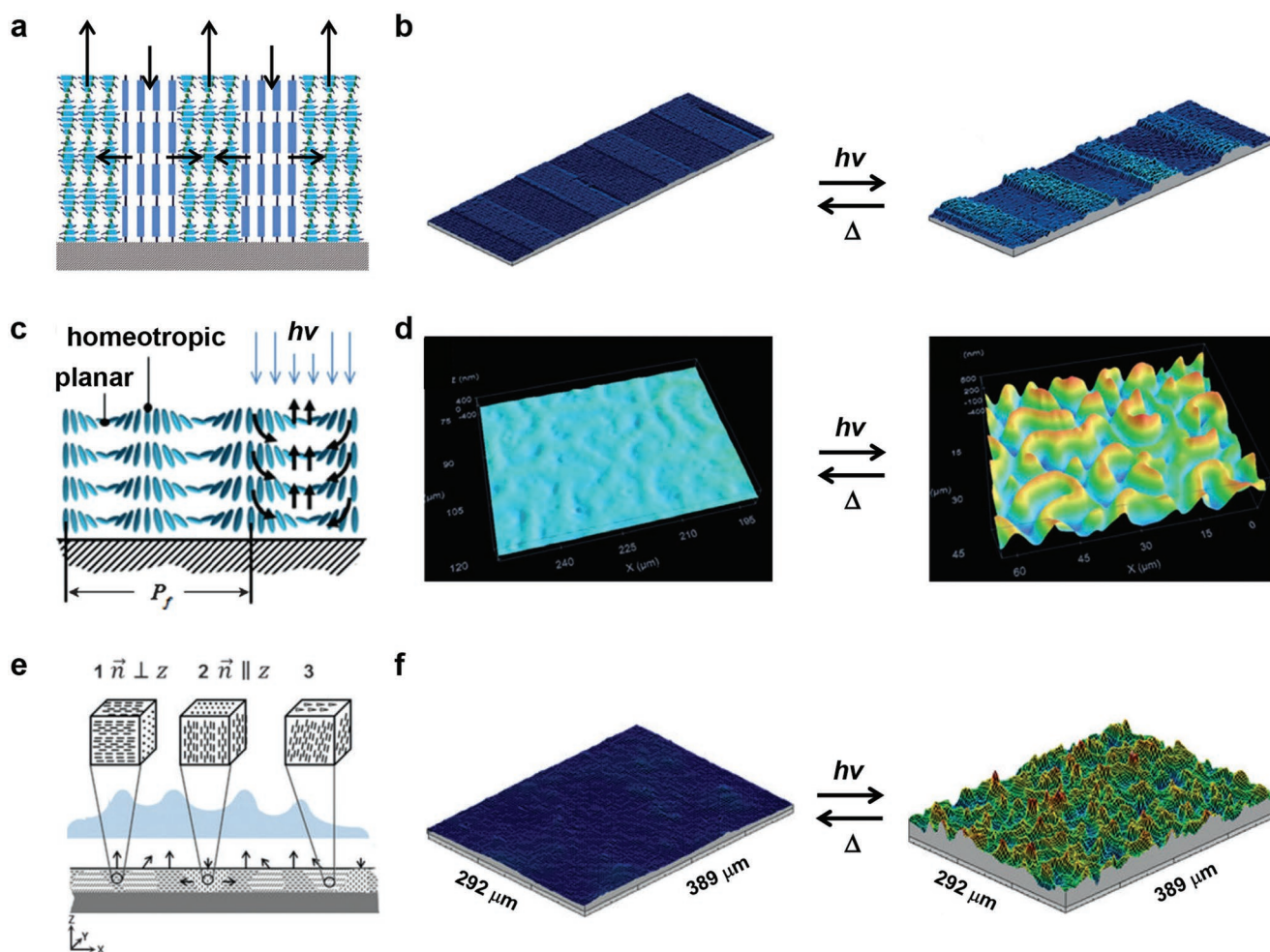


Figure 5. a) CLCP-containing striped patterns of alternating areas with chiral nematic order and homeotropic orientation. b) 3D images of surface topologies at the original state (left) and during illumination with UV light (right). a,b) Reproduced with permission.^[67] Copyright 2012, Wiley-VCH. c) Schematic representation of the dynamics of the fingerprints. d) 3D images of the initial flat state (left) and surface topographies under UV exposure (right). c,d) Reproduced with permission.^[69] Copyright 2014, Wiley-VCH. e) Schematic representation of the predicted deformation of the polydomain LC. From A, 1 to A, 3, molecules are aligned in 1) a uniaxial, 2) homeotropic, and 3) tilted manner. The arrows illustrate the direction of expansion propensities upon actuation and the blue inset illustrates the anticipated formation of surface structures. f) 3D images of the initial flat state (left) and UV activated surface topographies (right). e,f) Reproduced with permission.^[70] Copyright 2015, National Academy of Sciences.

light, each domain exhibited different deformation (Figure 5f). The planar domains tended to expand and deformed into hills, while the homeotropic domains expanded less or even formed valleys. Thanks to the dynamic creation of free volume, the photo-activated coating generated jagged surface topographies and showed a large depth modulation to the 24% of the film thickness.

In the all above-mentioned discussions, photo-induced reduction of molecular order in CLCP coatings produces free volume that results in the formation of dynamic surface topographies in a controlled manner. Furthermore, Broer and co-workers provided a new strategy of dual-wavelength exposure aiming for the enhancement of volume increase.^[71] Instead of involving solely 365 nm UV light to excite azobenzenes, authors triggered both *trans* and *cis* isomers of azobenzene by the introduction of a small proportion of 455 nm light or the addition of a small concentration of fluorescent dye to absorb UV light while emitting 455 nm light. The increased free

volume led to larger macroscopic surface deformations. It has been envisioned that this method provides a new insight in the photodeformation of azobenzene-containing LCPs.

3.3. Bending Movements

Due to the different degrees of contraction or expansion, the generated internal stress leads to the bending deformations, which are classified as the 3D movements (bending, walking, twisting, rolling, and oscillating) and are appealing for a wide range of applications. Ikeda et al. realized light-driven bending behaviors of azobenzene-containing monodomain LC gels and CLCP films by using the principle of asymmetric deformation.^[18] Upon irradiation with 366 nm UV light, CLCP films bent along the alignment direction of mesogens toward the light source and returned to the initial state when exposed to 450 nm visible light. At around 360 nm, most incident photons

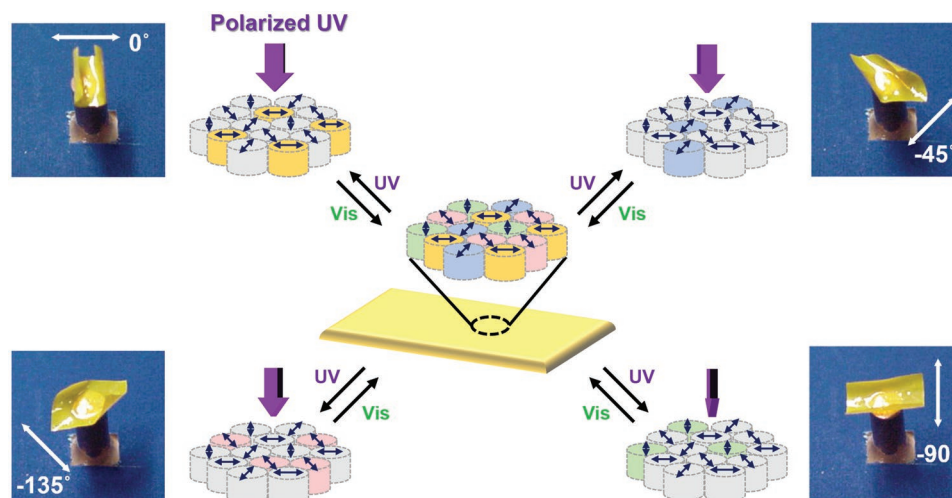


Figure 6. Photographs (Reproduced with permission.^[19] Copyright 2003, Springer Nature) and schematic (Reproduced with permission.^[34] Copyright 2011, Science Direct) of precisely direction-controlled bending of polydomain films induced by linearly polarized light.

were absorbed by azobenzene units that only existed in the surface region of CLCP films due to the large molar extinction coefficient of azobenzenes (about $2.6 \times 10^4 \text{ L mol}^{-1} \text{ cm}^{-1}$),^[34] which induced a stress gradient in the thickness direction of films, and thereby led to a bending deformation of the whole system. When this bent film was exposed to visible light, *cis*-azobenzenes went back to the *trans* state, turning mesogens in the surface layer of CLCPs from disorder into order.^[1,2]

In the work described above, the azobenzene-containing CLCPs give rise to a large light gradient subsequently resulting in an asymmetric actuation. This asymmetry occurs to be the key factor for the large deformation. The work of Ikeda and co-workers played a crucial role in the early development of light-driven actuators based on CLCPs. In the same year, they reported the directional bending of a polydomain CLCP film controlled by polarized light (Figure 6). In this case, azobenzene mesogens were aligned along one direction in each micro-sized domain even though the alignment of the whole system was random in the macroscopic view.^[19] Upon irradiation with linearly polarized UV light, the domains where azobenzenes aligned along the polarization direction absorbed light and contracted, resulting in the bending of the whole CLCP film parallel to the direction of the light polarization. This means that the bending direction of CLCP films can be controlled precisely and repeatedly just by changing the polarization direction of incident light.

Following these preliminary researches, efforts were devoted to investigate the key parameters influencing the bending deformation of azobenzene-containing LCPs, such as the crosslinking density,^[72–74] the spacer length of the monomer and crosslinker,^[75–77] the location of azobenzenes,^[78,79] as well as the LC alignment.^[80] Here, we focus on the effect of light wavelengths. Considering that UV light used for the actuation of CLCPs is not bio-friendly, the group of Yu has pioneered in the development of new LCP systems using visible light as a safer alternative trigger to induce bending behaviors. They developed 436 nm light-driven CLCPs that containing azotolane moieties in side chains for the first time. Owing to the long conjugated structure of the azotolane moiety, these CLCP films

produced bending/unbending behaviors upon visible light irradiation.^[81,82] To develop applications of light-driven CLCP actuators in possible biological systems, low-energy near-infrared (NIR) light instead of UV light is an ideal alternative because of the deeper penetration into tissues and less damage to biosamples. Yu et al. introduced lanthanide upconversion nanophosphors NaY-F₄:Yb,Tm into the azotolane-containing CLCP film and realized the fast bending upon exposure to continuous-wave NIR light at 980 nm. The main upconversion luminescence (UCL) emission peaks of the nanophosphors located at 450 and 475 nm, making it possible to trigger the *trans*–*cis* isomerization of the azotolane moieties.^[83] A new upconversion system with low-power excitation and little excitation photo-induced thermal effect has also been developed by Yu et al., they incorporated a red-to-blue triplet-triplet annihilation (TTA)-based system containing a sensitizer and an annihilator into a soft polyurethane film, and then laminated with an azotolane CLCP film, realizing a red-light-activated soft actuator driven by low-power-excited TTA-based UCL (TTA-UCL).^[84] Upon 635 nm light irradiation, the sensitizer/annihilator-containing film trapped the light and upconverted it into the blue TTA-UCL emission, and then the TTA-UCL was absorbed by the azotolane moieties via the emission-reabsorption procedure. The entire process induced the *trans*–*cis* isomerization of azotolane moieties and the alignment change of mesogens, which finally led to the bending deformation of the azotolane CLCP film. This work provides a potential biological application of LCP materials thanks to the negligible thermal effect and superior penetration ability into tissues of 635 nm laser.

The emergence of photo-induced bending deformation has stimulated researchers in the field to design and fabricate various soft actuators, exhibiting extensive applications of photo-deformable LCPs in artificial muscles,^[85] soft robots,^[28] smart surfaces,^[86] and other areas.^[87] A remarkable example was proposed by Ikeda et al. with a light-actuated plastic motor. This motor consisted of a laminated belt using an azobenzene-containing CLCP layer with the homogenous alignment as a coating on a flexible polyethylene (PE) supporting layer, and

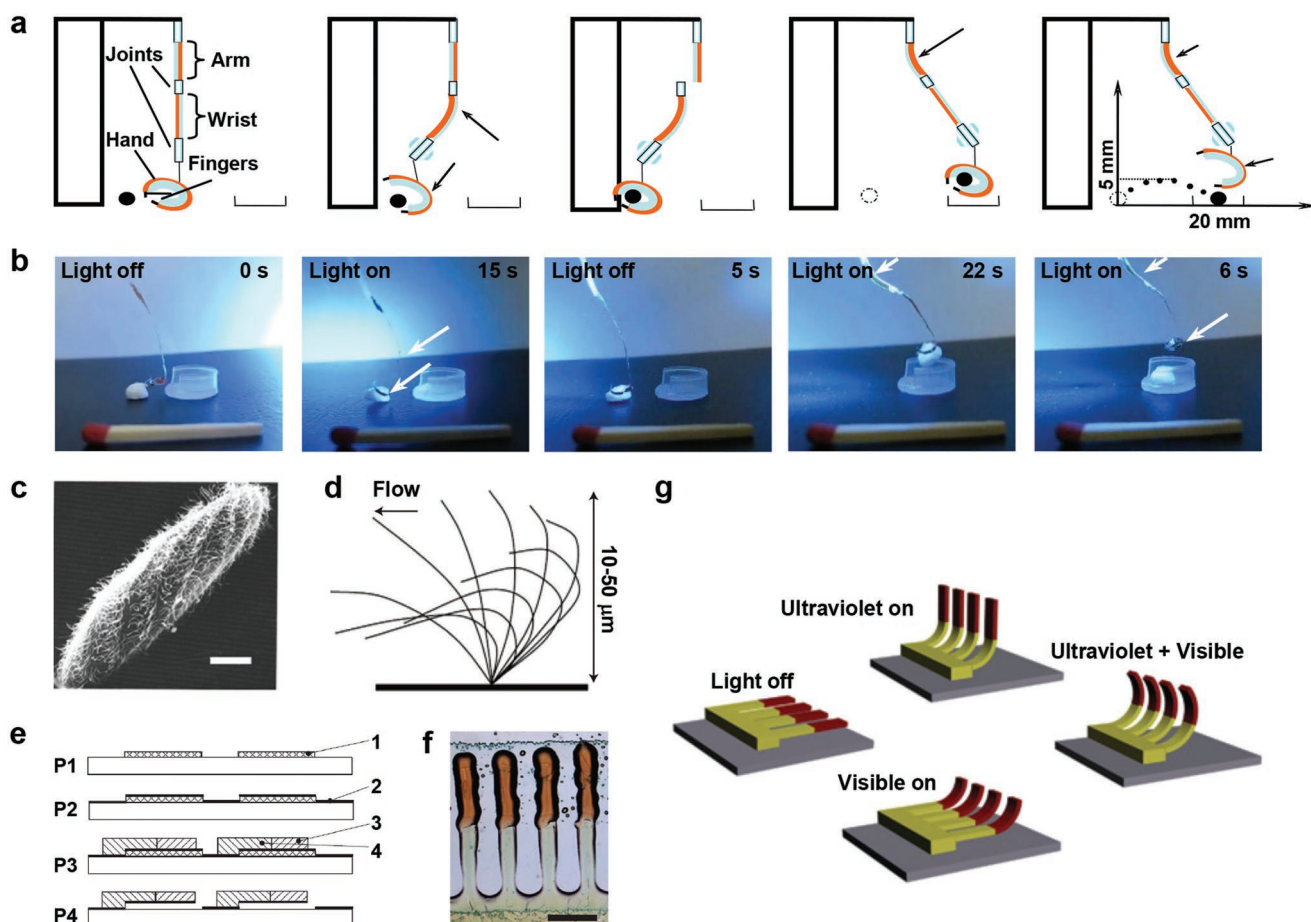


Figure 7. a) Schematic illustrations of the states of the microrobot during the process of manipulating the object. The insert coordinate indicates the moving distance of the object in vertical and horizontal directions. Arrows denote the parts irradiated with visible light for both (a) and (b). b) Photographs showing the microrobot picking, lifting, moving, and placing the object to a nearby container by turning on and off the light (470 nm, 30 mW cm^{-2}). Length of the match in the pictures: 30 mm. Thickness of PE and CLCP films: 12 mm. Object weight: 10 mg. a,b) Reproduced with permission.^[89] Copyright 2010, The Royal Society of Chemistry. c) Cilia can be found on several microorganisms, such as paramecia (scale bar 20 μm). d) A paramecium uses the beating motion of the cilia, characterized by different forward and backward strokes, for self-propulsion. e) Overview of the four basic processing steps to produce the modular cilia. P1, Structured deposition of the PVA release layer (1). P2, Spin-coating, curing and buffing of the PI alignment layer (2). P3, Inkjet deposition of the monomer mixtures containing two azobenzene chromophores (3) and (4) and curing. P4, Dissolving the PVA release layer. f) Microstructured cilia were made with two separate parts by separately polymerizing the two parts (scale bar 0.5 mm). g) Artificial, light-driven cilia produced an asymmetric motion controlled by the spectral composition of the light. c–g) Reproduced with permission.^[20] Copyright 2009, Springer Nature.

two pulleys.^[88] Irradiating the belt with UV and visible light at separated spaces induced the *cis/trans* states of azobenzenes and generated the consecutive contraction/expansion of the belt, rotating the motor continuously. This work realizes the sustained motion of LCPs using two light sources. Other types of 3D movements were also demonstrated by Ikeda group for laminated films composed of a homogeneously aligned CLCP layer and a PE film.^[31] They designed a curved CLCP laminated film with asymmetric end shapes prepared by an unstretched PE film partly laminated with a CLCP layer. This film moved forward in one direction as an inchworm walker upon alternate irradiation with UV and visible light. In addition, they also showed such 3D movements as a light-actuated flexible arm-like motion using the same CLCP/PE laminated film.

Photodeformable LCPs have received great interest for use as soft robotic devices, since they are ideal candidates for

realizing biomimetic movements by changing their shapes and dimensions. Engineering of the actuator, by means of cutting, bonding, etc. leads to functional devices. By engineering of a CLCP laminated film, Yu and co-workers developed a visible-light-driven plastic microrobot, which was able to carry objects in a predetermined manner (Figure 7a).^[89] In this case, the CLCP/PE bilayer films were employed as the “arm,” the “wrist,” and the “hand,” which guaranteed enough mechanical support and controlled bending directions; while the joint parts adopted the polypropylene to provide the requisite flexibility for the upper limb. Driven by light irradiation, this microrobot was manipulated to pick, lift, move, and place milligram-scale objects effectively, as illustrated in Figure 7b.

In nature, living creatures have developed a series of survival and self-protection strategies based on unique bending motions. For instance, cilia can be found at the surface of

many microorganisms, such as paramecia, they swim through a fluid flow by periodic beating of microscopic cilia that cover their surface (Figure 7c,d). Enlightened by these properties, van Oosten and co-workers designed a photoresponsive artificial cilia, which exhibited directional bending behaviors in response to light.^[20] The artificial cilia (10 mm × 3 mm × 10 μm) consisted of two different azobenzene dyes: one (yellow) was sensitive to UV light, the other (red) to the visible light. The two dyes were mounted at the top and the bottom of the actuator, respectively, which allowed for the sequential bending of different areas when switching the light wavelength (Figure 7g). This work successfully mimics the motion of natural cilia. In addition, ciliated surfaces in the respiratory tract of humans are used to sweep mucus.^[90] Broer et al. further fabricated an array of small parallel fibers based on a main-chain CLCP functionalized with coreactant azobenzenes by the pulling technique.^[91] These fibers with diameters of 70 μm placed side by side on a substrate bent toward the UV light in a concerted manner. When placed in a liquid, the cooperative bending movement of fibers created a flow to transport objects efficiently.

Except for the natural cilia, flytraps for instance, they close the leaves through the bending behavior upon mechanical triggers to prey on insects. Primagi et al. designed a light-actuated artificial flytrap which was capable of autonomous closure and object recognition.^[92] A thin layer of azobenzene-containing CLCP was responsible for the photoresponsiveness of the whole system. The use of the splay alignment as compared to uniaxial alignment allowed for larger bendings. By introducing an optical fiber that acted as a power source to transport the light energy, the photomechanical motion of CLCP film was triggered by reflected or scattered light from the environment. When a target object entered the field of view of this artificial flytrap, enough light was reflected back to the actuator surface, leading the CLCP film to bend and grip the object.^[49] In addition, there were some other bioinspired soft actuators based on the bending deformation of LCPs, such as artificial flower that imitated the natural flower's opening and closing,^[93] and artificial iris that mimicked the self-regulating behavior of the human iris.^[49]

3.4. Twisting and Rolling Actuations

Well-defined gradients in molecular alignment have been used to generate photo-induced deformations in LCPs. Besides uniaxial alignments (Figure 2a,b), more complex deformations have been reported by taking advantage of splay and twist aligned LCPs (Figure 2c,d). For example, the above-mentioned artificial cilia and flytrap actuators were based on splay aligned samples. The light-induced changes in this alignment generated different strains on the upper and lower surfaces of one monolithic layer, respectively, which resulted in larger bending deformations as compared to uniaxial alignments. For twisting movements of LCPs in response to light, several methods have been developed during the past decade. One is the use of chiral smectic C (SmC*) alignments. Ikeda and co-workers prepared novel SmC* ferroelectric CLCP films made from a mixture of acrylate molecules in the SmC* phase, which were highly oriented by applying an electric field combined with rubbing.^[94]

In the obtained ferroelectric CLCP films, the long axis of the molecules (director *n*) in each smectic layer was aligned in the same direction with a tilting angle with the rubbing direction (Figure 8a). Upon irradiation with 366 nm actinic light, the film bent toward the light source along the director *n* within 0.5 s. Owing to the tilting angle between the bending direction and the rubbing direction, the film even curled up to a corkscrew spiral shape (Figure 8b). Moreover, the photo-induced mechanical force generated in this process reached up to 220 kPa, close to the contraction force of human muscles (about 300 kPa).

As the preferred deformation direction depends on the orientation of the director, it is possible to create gradients in the local director axis across the thickness of the film.^[95] A twisted geometry, in which the orientation of nematic LC molecules changes by 90° from the bottom surface to the top surface of LCP films by the incorporation of chiral molecules, has been widely studied. The first example of light-driven actuators based on such alignment was reported by Broer and co-workers. They prepared CLCP films with a densely crosslinked, twisted configuration of azobenzene units.^[95] Although the networks were stiff and glassy at ambient temperature, the film cut at an angle of 45° between surface directors and the long axis of the film still rapidly coiled into a helical shape upon exposure to UV light, which was based on the twisted nematic configuration of LC alignment of 90°.

Similar twisting behavior is common in nature. For example, plant tendrils produce chiral twisting distortion under the stimuli of sunlight (Figure 8c).^[96] For diverse vine plants, winding stems may exist in two opposite directions. Inspired by this phenomenon, Fletcher et al. designed and synthesized a novel spring-like soft actuator composed of photoresponsive CLCPs (Figure 8e).^[21] Two chiral dopants were added to induce a left-handed and right-handed twist in the LC mixture, respectively. An azobenzene-based photoswitch which was incorporated into the polymer network via polymerizable acrylate groups underwent *trans-cis* isomerization upon exposure to UV light, resulting in a decrease of order parameter and then a macroscopic deformation. Photodeformation modes were fine-tuned by changing angles ϕ at which ribbons were cutting (Figure 8d). By adjusting cutting directions, various deformations were generated such as winding, unwinding, and helix inversion. In another contribution, they reported a long-lived twisting motion of CLCPs by using *ortho*-fluorinated azobenzenes as the photoswitch to increase the lifetime of photo-generated shapes and using the same chiral dopant as used in the foregoing work to promote a left-handed twisting motion of the film.^[97]

It should be mentioned that not only SmC* and twist-nematic configurations can be used to create twisting deformations. Indeed, large amplitude twisting deformations are also induced by light-driven release of stored elastic energies in LCPs derived from their nonuniform internal structures. And thus, no chiral molecules are required in these cases.^[32,96] Yang and co-workers demonstrated a polysiloxane-based CLCP actuator capable of performing bending and chiral twisting deformations through modulation of the light wavelength.^[96] The actuator consisted of two uniaxial aligned CLCP layers by covalently bonding together with overlapped angles of ± 45°.

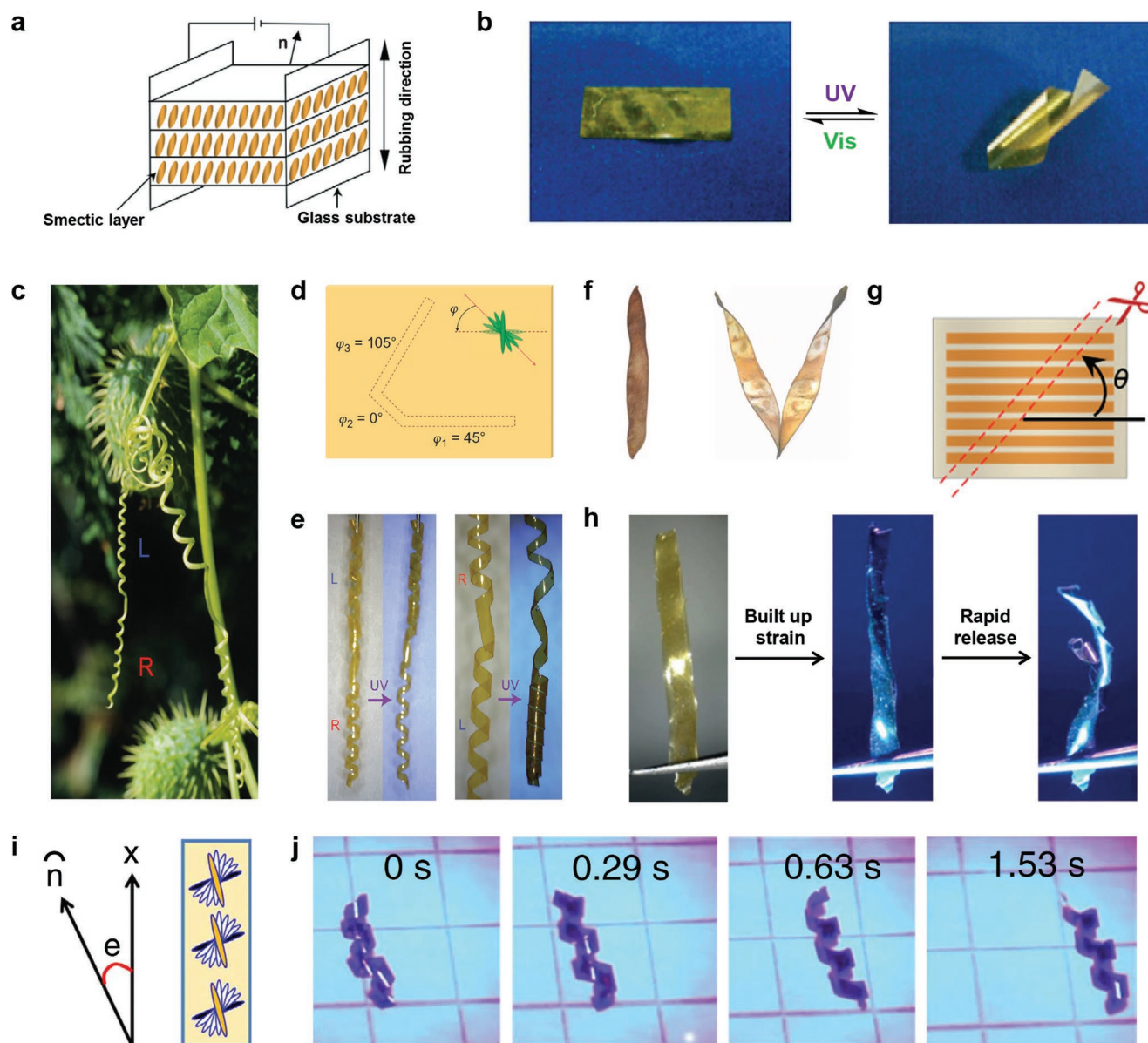


Figure 8. a) Azobenzene mesogens are aligned parallel to each other to form layers with a tilt between the director (\mathbf{n}) and the normal to the smectic layer that is parallel to the rubbing direction. b) Photographs of the ferroelectric CLCP film that exhibits bending and unbending behaviors upon alternative irradiation with UV (366 nm, 17 mW cm^{-2}) and visible light (547 nm, 110 mW cm^{-2}) at room temperature. a,b) Reproduced with permission.^[94] Copyright 2007, Wiley-VCH. c) A coiled tendril of the wild cucumber plant. d) The LCP film is cut to introduce regions that display different dynamic behaviors. e) A polymer spring that displays a cucumber tendril-like shape, composed of two oppositely handed helices connected by a kink. On irradiation, the right-handed helix unwinds (left) and the left-handed helix winds (right). c–e) Reproduced with permission.^[21] Copyright 2014, Springer Nature. f) Closed (left) and open (right) Bauhinia pods. Reproduced with permission.^[98] Copyright 2011, American Association for the Advancement of Science. g) The bar-patterned CLCP film can be cut with a variety of shapes depending on the cutting angle, which is the offset angle between the long axis of the ribbon and the orientation of the bars. h) The opening is mediated by the formation of a tube (18 s), as also observed in some biological systems. The artificial valves tend to twist in opposite directions, which builds up elastic energy (22 s) until the pod pops open from stress. g,h) Reproduced with permission.^[32] Copyright 2017, The Authors, published by Wiley-VCH. i) Schematic of the twisted nematic alignment in azo-CLCP strip. j) Photo-induced actuation of an azo-CLCP thin strip in the twisted nematic geometry aligns with the nematic director offset $+15^\circ$ (top) and -75° (bottom) to the principle axes of the strip. i,j) Reproduced under the terms of the CC BY 4.0 license.^[99] Copyright 2016, The Authors, published by Springer Nature.

The top layer was sensitive to both UV and NIR lights, and the bottom layer was only sensitive to NIR light. Upon irradiation with UV light, the CLCP ribbon bent toward the light source due to the different contraction ratios of the top and bottom

layers. Under the photothermal effect induced by NIR light, the CLCP ribbon showed helical curling motions since the nonuniform contractions created in the two-layer-overlapped region made an inclined angle with the long axis of the film. This

work successfully mimics the plant tendril with two different 3D reversible transformations, which is difficult to achieve from single-layer actuators. In addition, the similar strategy was utilized to mimic the opening of chiral seedpods (Figure 8f).^[98] Fletcher et al. developed an artificial seedpod based on the opposite work of a pair of springs.^[32] Using photo-patterning method, they prepared azobenzene-containing CLCP films with alternating bars, i.e., the highly ordered bars with uniaxial alignments and the lower ordered bars. Under UV light illumination, the *trans*–*cis* isomerization of azobenzenes occurred in the highly ordered bars and induced an elongation of the bars. Photoisomerization also occurred in the disordered bars but was not magnified into the macroscopic deformation effectively. In this process, the strain built up slowly in the form of elastic energy and was released in an ultra-fast motion. Varying the angle at which the ribbons were cut could control the amount of strain that accumulated (Figure 8g). Two mirror-image ribbons were cut to mimic the valves of an artificial seedpod. When irradiated with UV light, the ribbons twisted into springs to compensate internal strains, and the pod opened (Figure 8h).

The group of White developed an azobenzene-containing CLCP film capable of twisting and rolling movements.^[99] With the continuous irradiation of 320–500 nm wide-wavelength light, the strip first twisted into a spiral actuator and then rolled in the direction of offset angle (the angle between the director and the long axis of strip) (Figure 8i). The mechanism of the rolling movement was: the *trans*–*cis* and *cis*–*trans* bidirectional isomerization reaction induced by wide-wavelength light generated a strain gradient across the film thickness. The strain gradient was further enhanced by the twisted nematic alignment of azobenzene-containing CLCP strip. Due to the offset angle, the strip thereby produced a twisting behavior. By means of the friction between the actuator and the desktop, a driving force was generated, which was capable to impulse the center of gravity of the spiral actuator to roll (Figure 8j). This work clearly elaborates the mechanism of photo-controlled rolling motion of the spiral actuator and explains how three key factors of photo-induced stress gradient, friction, and rolling resistance affect the rolling behavior, which help us thoroughly understand the conversion process of light energy into mechanical motions.

4. Improvement of Materials

Until now, a variety of azobenzene-containing LCP actuators in the form of films or fibers have been developed. In these systems, the existence of an appropriate level of crosslinking networks plays an important role for macroscopic deformations because it is responsible for the accumulation of the photomechanical force generated from the azobenzene mesogens across the entire network.^[100] However, LCPs with chemically crosslinked networks are insoluble in organic solvents and infusible upon heating, which makes them incompatible with commonly used polymer processing methods.^[101,102] This poor processing performance limits for the further applications and developments of photodeformable LCPs. Therefore, the molecular design of new materials is essential for improving the processing performance of LCPs.

4.1. Post-Crosslinked LCPs

Recent years have witnessed an effective strategy of yielding photoresponsive LCP-based actuating materials using post-crosslinking reaction. These materials possess crosslinkable groups, allowing for the formation of chemical or physical networks and the fixation of the shape after molding. Till now, there have been reported several ways of implementing post-crosslinking reaction. One of them is the crosslinking reaction between the hydroxyl groups and the isocyanates. Ikeda et al. reported the precise directional control of photomobility in CLCP fibers.^[103] These CLCP fibers were prepared by two-step reactions, which involved the first synthesis of an uncrosslinked side-chain copolymers bearing a hydroxyl-substituted azobenzene mesogen by the radical polymerization and the subsequent quickly pulling of its mixture with the crosslinker (4, 4'-methylenebis (phenyl isocyanate)) with a tip of a toothpick upon heating. Irradiation with 366 nm light caused the fibers to bend toward the actinic light source, and the direction of bending was controlled by changing an irradiation spot of the fibers. In the aforementioned work, the fiber-drawing process occurs simultaneously with the fast crosslinking reaction, thus it is difficult to fabricate CLCP fibers with well-controlled properties. Using the similar crosslinking reaction, Yu et al. recently demonstrated LC random copolymers with azobenzene and biphenyl groups in the side chain.^[104] While in this work, the crosslinked fibers were obtained through first fabrication of uncrosslinked fibers by quickly drawing out from the melted copolymer upon heating and then the immersion in a solution of the crosslinker (hexamethylene diisocyanate) to complete crosslinking. By using this method, the azobenzene-containing CLCP fibers with easily controlled diameters and high alignment order were obtained. The CLCP fibers containing different azobenzene concentrations and crosslinking densities exhibited reversible bending behaviors with the direction away from the UV light.

Another commonly used strategy in the post-crosslinked systems is based on the side-chain LCPs bearing *N*-hydroxysuccinimide carboxylate-substituted azobenzene mesogens. Zhang and co-workers first synthesized a series of photoresponsive side-chain LCPs with an *N*-hydroxysuccinimide carboxylate-substituted azobenzene mesogen, which could be easily crosslinked with a difunctional primary amine under mild conditions.^[105] By using these post-crosslinkable LC homopolymers or copolymers, they further demonstrated the photo-induced diffraction efficiency of surface relief gratings^[106] and UV-light-driven bending behaviors of fibers.^[107] Based on this post-crosslinking reaction, Yu et al. incorporated a soft poly(ethylene oxide) (PEO) block into the system and synthesized a reactive block copolymer PEO-*b*-PAZO (Figure 9a).^[108] The introduction of PEO provided enough free volume for the photoisomerization of azobenzenes and photochemical phase transition, leading to excellent photodeformation of CLCP fibers and films. The uncrosslinked fibers and films were first obtained by thermal-drawing and solution casting methods, respectively, and then they were immersed in a solution of crosslinker 1,6-hexanediamine to complete the post-crosslinking reaction (Figure 9b). Based on the same method, the azotolene-containing CLCP fibers and films have also

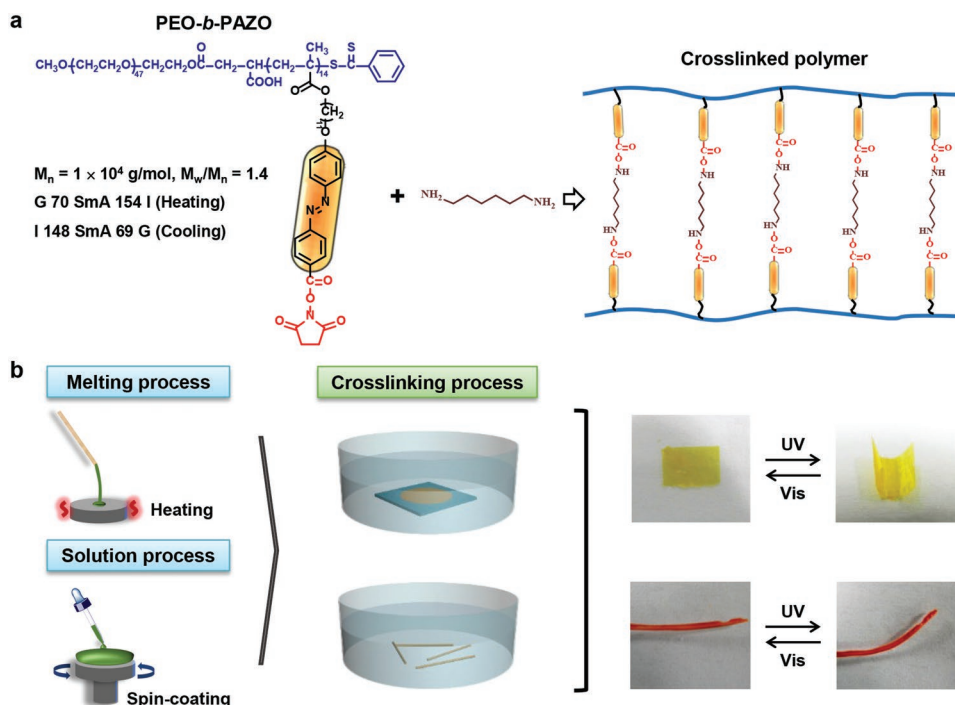


Figure 9. a) Chemical structures of PEO-*b*-PAZO and crosslinker 1,6-hexanediamine, and the crosslinking route. Reproduced with permission.^[108] Copyright 2015, The Royal Society of Chemistry. b) Preparation processes and the reversible bending behaviors of post-crosslinked films and fibers. Reproduced with permission.^[109] Copyright 2016, American Chemical Society.

been developed, showing photo-induced bending behaviors in response to visible light.^[109] Except for these contributions, they also fabricated composite light-actuated films by combining a crosslinkable LCP with commercially available polyurethane via a simple blending method, which reduced cost and enlarged the scope of applications of CLCPs.^[110]

4.2. CLCPs with Exchangeable Covalent Bonds

Another strategy to produce the photoresponsive LCPs is based on dynamic covalent bonds.^[111] Dynamic covalent bonds are covalent bonds capable of switching or exchanging between several molecules autonomously or in response to stimuli.^[112] The introduction of dynamic bonds into LCP materials provides them with unique properties such as reshaping, self-healing, and shape memory properties. For example, Zhang et al. demonstrated the synthesis of side-chain LCPs bearing pendant thiol-substituted azobenzenes and their fibers with the advantages of both chemically and physically crosslinked light-driven actuating systems.^[100] By reversible switches between thiol and disulfide groups via redox reactions, the photodeformable fibers showed high recyclability.

Besides the switching between two molecules, exchangeable covalent bonds which allow for the breaking and reformation of covalent bonds without changing the total number of crosslinks have also received significant attention. Herein, we will focus on the employment of exchangeable covalent bonds in LCP systems. The exchangeable covalent bonds reported for LCPs mainly come from ester,^[102,113–117] disulfide,^[118] and allyl

sulfide groups.^[33,119–121] Transesterification is a dynamic reaction occurs between an ester bond and a hydroxyl group within the polymer backbone, and this usually requires elevated temperatures and catalysts (Figure 10a).^[112] At temperatures greater than or equal to the isotropic transition temperature, the covalent bonds between hydroxyl and ester groups break apart and reform elsewhere. This process allows monodomains to be programmed or erased after polymerization has occurred.^[122] Ji et al. designed CLCPs with exchangeable links (xCLCPs), which showed thermal-induced deformations similar to the traditional CLCPs with permanent network crosslinks.^[102] These xCLCPs were moldable, allowing for easy processing and alignment, and were altered through remolding with different stress patterns. In addition, they introduced carbon nanotubes (CNTs) into xCLCPs, realizing the photo-induced transesterification under the action of photothermal effect of CNTs.^[115,116,123] As a result, these CNT-xCLCPs were welded, reshaped, and healed upon light irradiation.

Ikeda and co-workers further combined transesterification with photoresponsive CLCPs, enabling the reshaping after the formation of polymer networks and photo-induced deformation upon light irradiation.^[113] Particularly, no catalyst was required in this exchange reaction due to the high reactivity of phenyl-OH groups. A spiral ribbon was reshaped from a monodomain film by rolling it around a rod at 120 °C (Figure 10b). The alignment of mesogens was achieved by stretching and fixed by rearrangement of network topology. Upon irradiation with UV and visible light from outside of the sample, the ribbon contracted along the stretching direction to unwind and recovered to the winding state, respectively (Figure 10c,d). Recently, Zhao

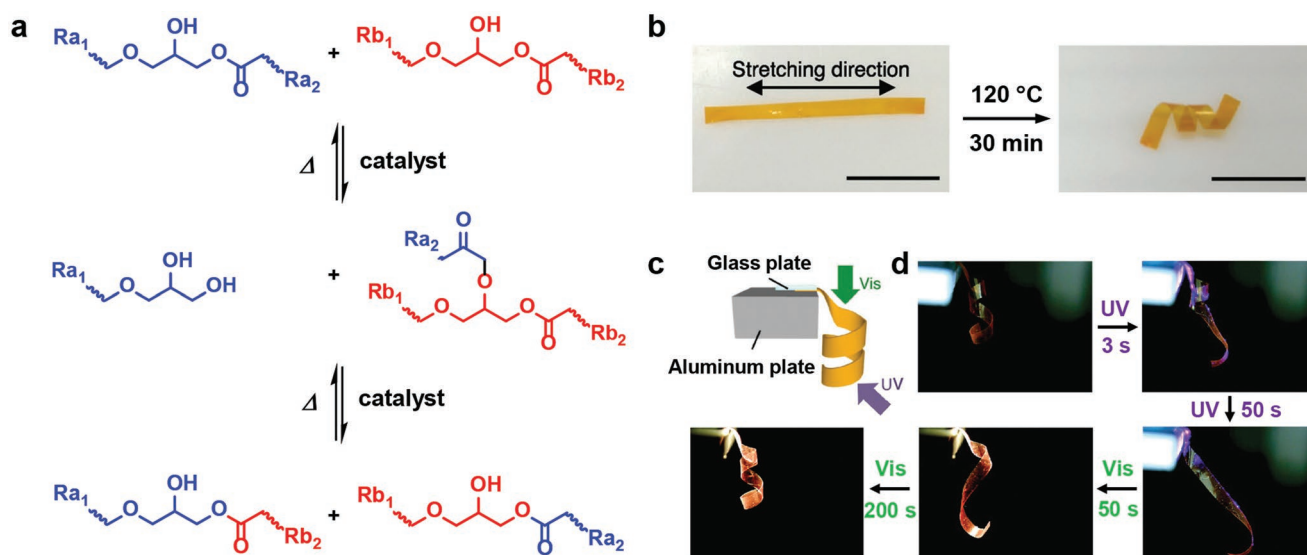


Figure 10. a) Schematic illustration of the reversible transesterification reaction. Reproduced with permission.^[124] Copyright 2017, Wiley-VCH. b) Reshaping of a monodomain CLCP film into a spiral ribbon. Scale bars: 10 mm. Size of the film before reshaping: 25 mm × 2 mm × 70 μm. c) Experimental setup for the observation of photo-induced deformation of the spiral ribbon. d) Photo-induced deformation of the spiral ribbon upon irradiation with UV (365 nm, 97 mW cm⁻²) and visible light (>540 nm, 60 mW cm⁻²) at room temperature. b–d) Reproduced with permission.^[113] Copyright 2016, Wiley-VCH.

et al. reported photoresponsive malleable CLCP actuators by introducing exchangeable ester bonds.^[124] By applying a certain stress to the sample during processing, the mechanical strain energy was stored when the actuator was formed. When illuminated with UV light, not only a mechanical force upon the photoisomerization of azobenzene mesogens was generated but also the prestored strain energy had been released, which was a strategy for enhancing the photo-induced mechanical force. In the foregoing work reported by Ikeda et al., CLCPs were synthesized with polysiloxane as backbone and azobenzene moieties as side-chain crosslinkers. Here, CLCPs bearing an epoxy-acid-derived rearrangeable network with azobenzene moieties positioned in the chain backbone enable large contraction force upon photo-induced release of stored strain energy.

The above-mentioned transesterification reaction generated a rearrangeable network structure that improved the reprocessability of the material. Besides transesterification, disulfide bonds are another form of exchangeable covalent bonds that allow reprogramming and recycling of CLCPs. Generally, disulfide exchanges follow either radical or anionic pathways. In the radical pathway, the thiol-disulfide bonds fragment when exposed to UV light irradiation or thermal stimuli, allowing them to reform bonds with other thiol-disulfides (Figure 11a). Cai et al. developed a reprogrammable, reprocessable, and self-healable CLCP with exchangeable disulfide bonds.^[125] The CLCP was reprogrammed from the polydomain state to the monodomain state by heating or UV irradiation (Figure 11b), due to the rearrangement of the polymer network induced by the metathesis reaction of disulfide bonds. Using the monodomain CLCP, they demonstrated the reversible contraction/expansion of films and micropillars upon heating and cooling. In addition, disulfide exchanges can follow anionic way. The attack of a thiolate anion at a disulfide bond results in the formation of a new disulfide bond and thiolate anion via heterolytic cleavage of the S-S bond, where the thiolate anion is generated under basic conditions

or by addition of catalysts (Figure 11c).^[112] Kessler et al. integrated thermal-responsive LCs, azobenzenes, and exchangeable disulfide bonds into an LC epoxy network, allowing for the resulting material with shape memory properties and photo-mechanical behaviors.^[118] Using a monothiol, the thiol-disulfide interchange reaction was initiated and formed a new disulfide and a thiol, enabling CLCP be reshaped, repaired, and recycled.

Except for networks with ester and disulfide groups, allyl sulfide groups are also promising to control alignment and birefringence of chemically crosslinked LCPs. Ji et al. reported tubular soft actuators with complex movements based on a CLCP with allyl sulfide groups.^[120] Allyl sulfide groups located in the backbone of CLCPs were sensitive to free radicals. Radicals generated from photoinitiators during UV light exposure activated the addition-fragmentation chain transfer between allyl sulfide groups, leading to the topological changes of CLCPs (Figure 11d). When an external force was applied at the same time, the macroscopic alignment of LC was established and remained after turning off the UV light. The alignment of CLCP tubular actuators was locally programmed by light irradiation at any specific region, enabling the site-specific introduction of different modes of deformation into one actuator. It was worth noting that the alignment was erased easily by stress relaxation at the isotropic state by UV light and regained by tension. The reverse process (memory of aligned states through exchange reaction of allyl sulfide) was also demonstrated by the research from the Bowman group, allowing for shaping with light and actuation by temperature change (Figure 11e).^[119]

4.3. Linear LCPs

Processing performance has been improved for the above-mentioned materials, but still suffers from a limitation in the incompatibility with existing industrial processing methods

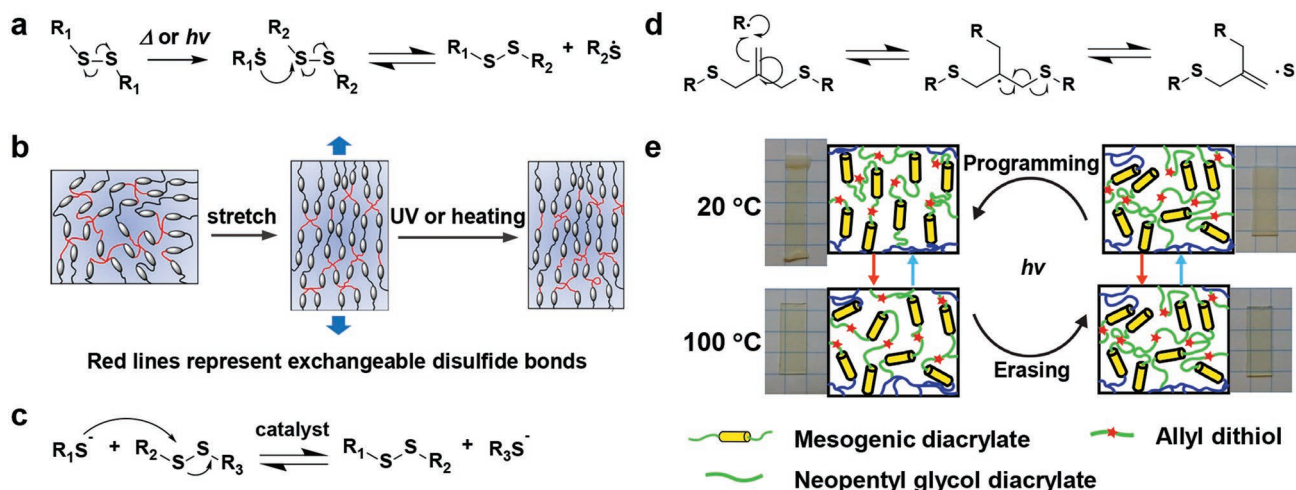


Figure 11. a) Disulfide exchanges in radical pathways. b) Reshaping mechanism of dynamic network of the CLCP under UV irradiation or upon heating. Reproduced with permission.^[125] Copyright 2017, American Chemical Society. c) Disulfide exchanges in anionic pathways. a,c) Reproduced with permission.^[112] Copyright 2019, Wiley-VCH. d) Schematic of radical-mediated allyl sulfide bond exchange mechanism. The radicals are generated through light-facilitated cleavage of a photoinitiator. Reproduced with permission.^[121] Copyright 2017, Wiley-VCH. e) CLCPs are aligned and subsequently erased by applying a mechanical bias (programming) or a thermal disruption (erasing) coupled with light ($h\nu$, 30 mW cm⁻², 320–500 nm). Reproduced with permission.^[119] Copyright 2018, The Authors, some rights reserved; exclusive licensee American Association for the Advancement of Science. Distributed under a CC BY-NC 4.0 license, published by American Association for the Advancement of Science.

due to the presence of chemical crosslinking networks. Lee et al. synthesized the azobenzene-containing linear LCs (LLCPs) via acyclic diene metathesis polymerization.^[126,127] Without the chemical crosslinks, the nematic LLCP fibers and films were fabricated via melt-spinning and solution-casting methods, respectively, and showed bending and unbending behaviors by exposing to UV and visible light. However, then low molecular weight (only about 10⁴ g mol⁻¹) of the obtained LLCPs resulted in a linear decline in mechanical properties of actuators. It remains a great challenge to design LLCPs with robust mechanical properties.

Nature provides countless inspirations for devising mechanically robust materials. Arteries are natural tough bioactuators, which are capable of withstanding impressive pressure stress and displaying rupture strengths up to 2000 mm Hg. The robust mechanical property originates from the lamellar structure and the composite composition of an artery wall (Figure 12a). Inspired by the lamellar structure of artery walls, Yu and co-workers designed a novel LLCP ($M_n \approx 3.6 \times 10^5$ g mol⁻¹, $\mathcal{D} \approx 1.86$) based on the assembly characteristic of LCs, as shown in Figure 12b.^[30] In order to prepare high-molecular-weight LLCPs and improve the mechanical robustness of materials further, the ring-opening metathesis polymerization (ROMP) as a living polymerization method was employed to synthesize this LLCP. The rubber-like main chain was responsible for viscoelasticity, affording robust mechanical property for the material. Azobenzene mesogens in side chains acted as “photonic muscles,” endowing the material with photodeformability. Long spacers were used to connect azobenzene mesogens with the main chain, offering enough freedom for mesogens to self-assemble into a highly ordered lamellar structure at the nanoscale.

A salient feature of the newly designed LLCP is the high mechanical robustness, which is ascribed to the ordered

lamellar structure and the high molecular weight. This LLCP is soluble and fusible because of the linear structure, and can be processed and molded by traditional melting and solution processing methods (Figure 12c). Besides, the self-assembly ability of the mesogens in LLCP simplifies the orientation process. Omitting additional alignment steps such as mechanical stretching, rubbed alignment layer, or magnetic field, etc., the highly ordered smectic phase of the LLCP is easily obtained by annealing.

Based on above research, they further designed a novel linear LC copolymer (PABBP, $M_n \approx 3.0 \times 10^5$ g mol⁻¹, $\mathcal{D} \approx 1.67$) combining the photoresponsive azobenzenes and biphenyl moieties by ROMP method (Figure 12d).^[128] The flexible backbone and long spacers of the copolymer PABBP provide enough free volume for the co-assembly of the azobenzene and biphenyl mesogens, which have the similar molecular size. Similar to the above-mentioned homopolymer, two kinds of mesogens in the drop-casting copolymer film co-assembled into an ordered lamellar structure upon annealing, endowing the material with moderate modulus. In addition, the incorporation of biphenyl mesogens increases the light penetration depth in the PABBP layer and enhances its photodeformability due to the reduction of the azobenzene content. The excellent photodeformability, self-assemble ability, and moderate modulus make PABBP suitable to serve as the deformable layer to construct the bilayer photo-controllable flexible microtube (PFM). The PFM possessed a bilayer structure, including an outer flexible supporting layer and an inner photodeformable LLCP layer (Figure 12e,f). The commercially available ethylene-vinyl acetate (EVA) copolymer microtube was chosen as the supporting layer to assemble the PFM for its good flexibility and comparable modulus. As a result, the PFM was facilely programmed into various shapes due to its good flexibility (Figure 12g).

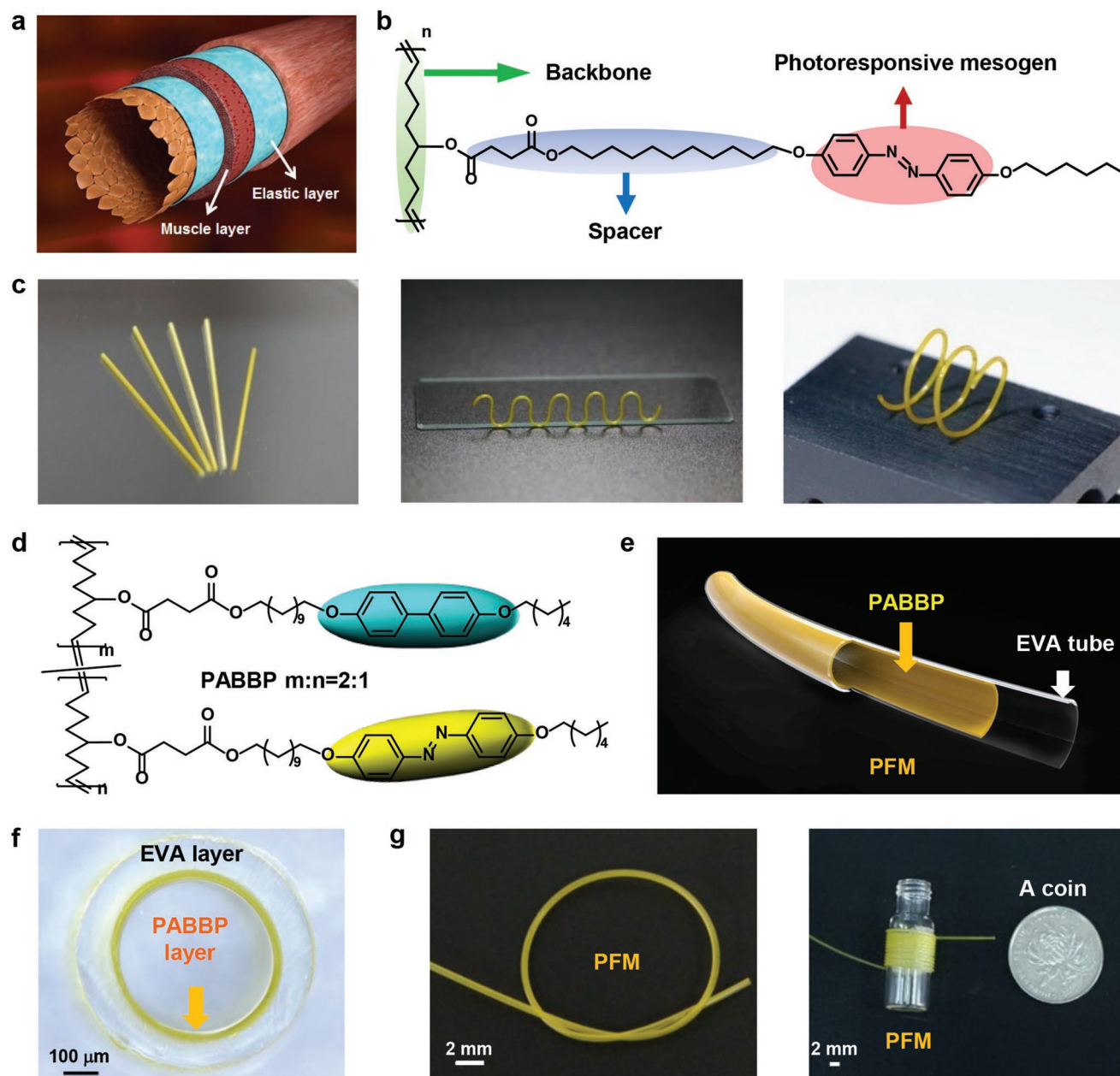


Figure 12. a) Schematic illustration of the multilayer structure of artery walls. b) Molecular structure of the LLC. c) Photographs showing left to right a batch of freestanding straight, serpentine, and helical TMAs. The serpentine TMA is leaning against the edge of a glass slide. The inner diameter of the straight TMAs is 0.5 mm, and that both of serpentine and helical TMA is 0.6 mm. The wall thickness of all the TMAs is $\approx 8 \mu\text{m}$. Reproduced with permission.^[30] Copyright 2016, Springer Nature. d) Chemical structure of the PABBP copolymer. e) Schematic representation of the bilayer structure of the PFM. f) Cross-section image of the PFM. The outer and inner diameters of the EVA microtube are ≈ 600 and $\approx 400 \mu\text{m}$, respectively. The EVA layer is $\approx 100 \mu\text{m}$ thick and the PABBP layer is $\approx 25 \mu\text{m}$ thick. g) Photographs of the knotted (left) and coiled (right) PFMs showing good flexibility. Reproduced with permission.^[128] Copyright 2019, Wiley-VCH.

5. Processing Techniques of CLCP Actuators

5.1. Fabrication of Film-Based CLCP Actuators

Light-driven CLCPs are promising in a wide range of macro- and microscaled actuators.^[1,129] Depending on the geometry of the final materials (fibers, films, tubes, particles, etc.), different types

of actuators have been fabricated. Until now, the large majority of CLCP macroactuators are prepared based on films. The processing is a critical step to promote CLCPs from fundamental researches in the laboratory toward practical applications. The fabrication of CLCP films generally requires the macroscopic alignment of LC mesogens. All the processing methods are tailored according to the intrinsic properties of materials. Two processing

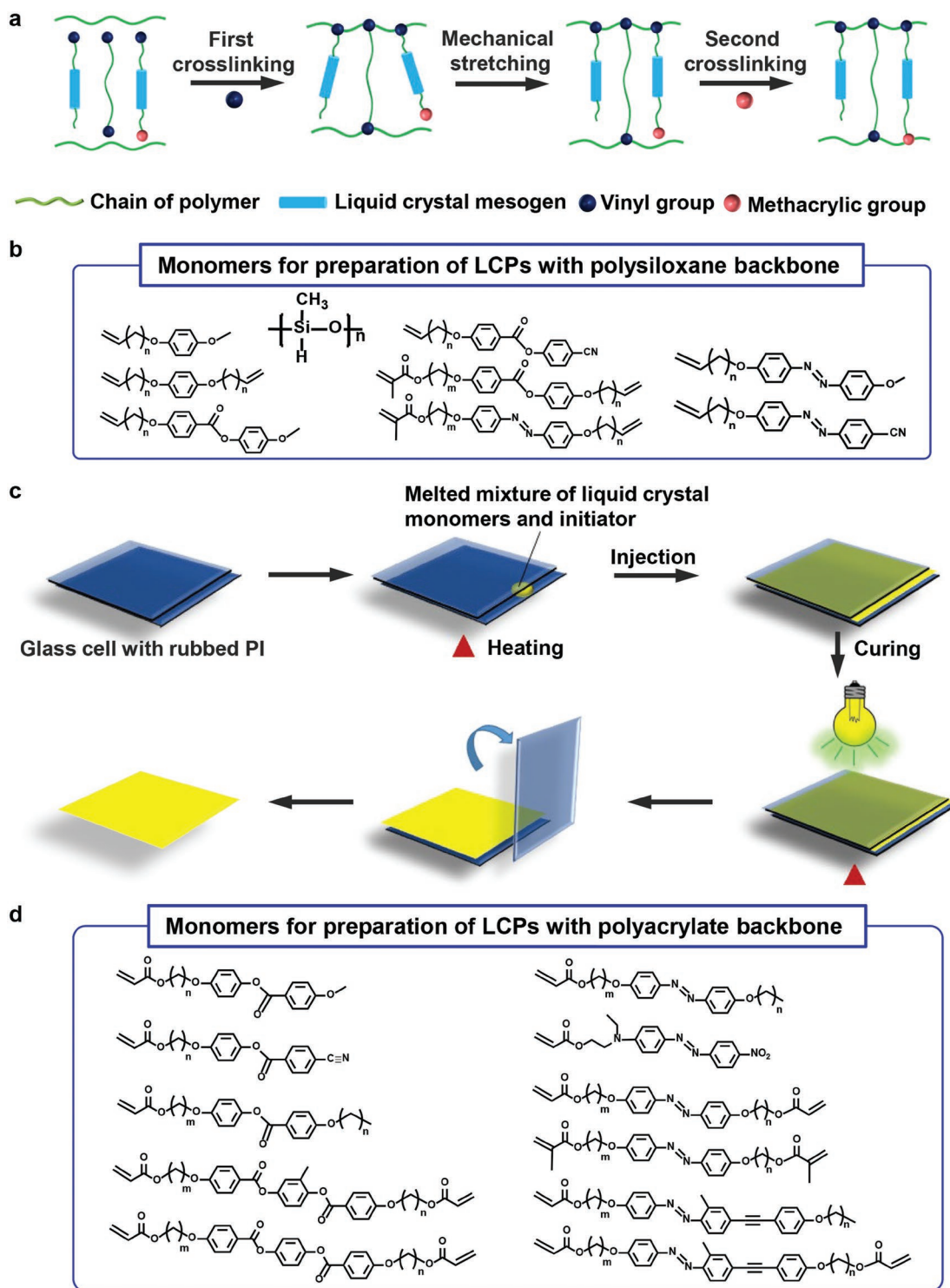


Figure 13. a) Schematic illustration of the two-step method used to prepare CLCPs. Reproduced with permission.^[130] Copyright 1991, Wiley-VCH. b) LC monomers used to prepare LCPs with the polysiloxane backbone. c) Schematic illustration of the one-step method used to prepare highly oriented LC side-chain polymers. Reproduced with permission.^[8] Copyright 2017, Acta Polymerica Sinica. d) LC monomers used to prepare LCPs based on the acrylic backbone.

methods that have been widely adopted to fabricate CLCP films are the two-step method and the one-step method,^[1,26] which are created based on properties of siloxane CLCPs^[130,131] (Figure 13b) and acrylic CLCPs^[31,57,67,79,80,88,94,132–136] (Figure 13d), respectively.

Two-step method is commonly used to synthesize siloxane monodomain CLCPs (Figure 13a).^[17,77,130,137–144] It is first achieved by using a linear and nonfunctional polyhydrosiloxane chain, which is coupled with mesogenic groups and

a crosslinking agent in one step. The platinum-catalyzed addition of terminal C=C bonds to the Si-H bonds is used to attach the mesogens and crosslinking moieties to the polyhydrosiloxane chain. Kinetic measurements showed that the vinyl groups reacted two orders of magnitude faster than methacryloyl groups, which allowed the crosslinking to occur in two steps.^[130] Well-defined weak networks are prepared in the first step by the reaction of vinyl groups. These weakly crosslinked networks are then stretched with a constant load to induce network anisotropy. In the second reaction step, the slower reaction of the methacryloyl groups further fixes the network anisotropy.^[141,145–147] With the necessity of mechanical stretching, this method is normally applied to fabricate CLCP films with macroscopic monodomain alignments.^[96]

One-step method is one of the fabrication techniques of LC film actuators developed by Broer et al. in the 1980s (Figure 13c). Typically, the mixtures of LC monomers with low viscosity are suitable for this method to prepare monodomain CLCP films. The molten LC monomers are first injected into an LC cell coated with a rubbed polyimide (PI) alignment layer by the capillary force, and are arranged in the preferred rubbing direction due to the surface anchoring effect. Finally, highly ordered structures of LCs are fixed by thermal- or photo-polymerization.^[148] A major advantage of this method lies in its ability to manipulate LC alignments, such as homogeneous,^[18] homeotropic,^[80] splay,^[25] patterned^[62] alignments (Figure 2), etc.

5.2. Fabrication of CLCP Microactuators

The above-mentioned methods are generally used for the preparation of CLCP actuators in macroscopic scale. Following on the trend of miniaturization found in many fields of materials science, a variety of processing techniques have been developed in the fabrication of CLCP microactuators, such as inkjet printing,^[20] DLW,^[28] replica molding,^[27] etc. These processing methods allow the CLCPs with good deformation properties as traditional processing methods, and enable them to be processed into various kinds of microactuators, such as artificial cilia,^[20] microwalkers,^[28] and other devices.

5.2.1. Inkjet Printing

Inkjet printing is a material-conserving deposition technique used for liquid phase materials, which offers resolutions in the micrometer range.^[149] van Oosten et al. developed microactuators by employing the microelectronics assembly technology combined with the inkjet printing (Figure 7c–g).^[20] The inks containing monomeric LC mixtures were deposited on the PI layer by an inkjet printer and were photo-polymerized to obtain cilia-like arrays with splayed alignments by dissolving the sacrificial polyvinyl alcohol (PVA) layer. The inkjet printing technique allows variations of the material composition in the plane of the substrate in a single processing step. Therefore, the selection of multiple inks

provides separate control for each subunit in this actuator by different activation light.

5.2.2. DLW

DLW technique is generally used to pattern the complex 3D hybrid robot structures with submicrometer scale resolution by a well control of sample position and laser exposure condition.^[28] In recent years, this method has proven to be a powerful tool for the preparation of CLCP microactuators.^[28,150,151] During the writing process, the LC monomers are crosslinked by scanning the laser beam, and the microstructures maintain the desired molecular orientation.

For instance, Wiersma et al. prepared a microrobot by employing the DLW system, which walked in response to light.^[28] The special design of microwalker's legs, which were cone-shaped with the angular inclination, effectively reduced the adhesion between legs and the contact surface. Importantly, this microscopic walker absorbed light directly from the surroundings with no need to target specific individual parts with a light beam. This preparation technique provides great prospect for applications in microphotonics and robotics of CLCPs.

5.2.3. Replica Molding

Patterned structures on surfaces are of considerable importance in many areas such as microelectronics, information storage, microfluidics, etc. A wide range of techniques have been developed to prepare micrometer- or even nanometer-sized structures. In particular, replica molding, which is based on a soft polymer mold such as poly(dimethylsiloxane) (PDMS) has been widely employed thanks to its low demand in equipment, simple operation, and low cost. The replica molding technique includes three steps as illustrated in Figure 14a: 1) fabrication of a patterned silicon template with desired dimensions; 2) generating a negative PDMS replica from the original silicon template as a mold; 3) filling the PDMS mold with the liquid precursor, followed by curing and peeling off to obtain the patterned structures. By using this method, Keller et al. fabricated the microarray of a main-chain CLCP.^[27] A strong magnetic field was applied to align the nematic director parallel to the long axis of pillars. Each pillar showed an ultra-large and reversible contraction of 400% when heated at a temperature close to nematic-isotropic phase transition of the CLCP. The micrometer-sized actuator discussed here is only heat sensitive. To fabricate photoresponsive CLCP micropillars, it is necessary to select an appropriate photoinitiator to effectively induce the polymerization of photoresponsive monomers. To circumvent this difficulty, Yu et al. employed a visible-light initiator to prepare photoresponsive azobenzene-containing CLCP micropillar arrays by using the secondary replication method, owing to the strong absorption of azobenzenes in the UV region.^[152] The microarrayed film showed reversible switch of superhydrophobic adhesion by alternating illumination of UV and visible light.

Omitting the steps to prepare soft templates, Yu et al. fabricated a 2D photonic crystal of azobenzene-containing CLCPs in

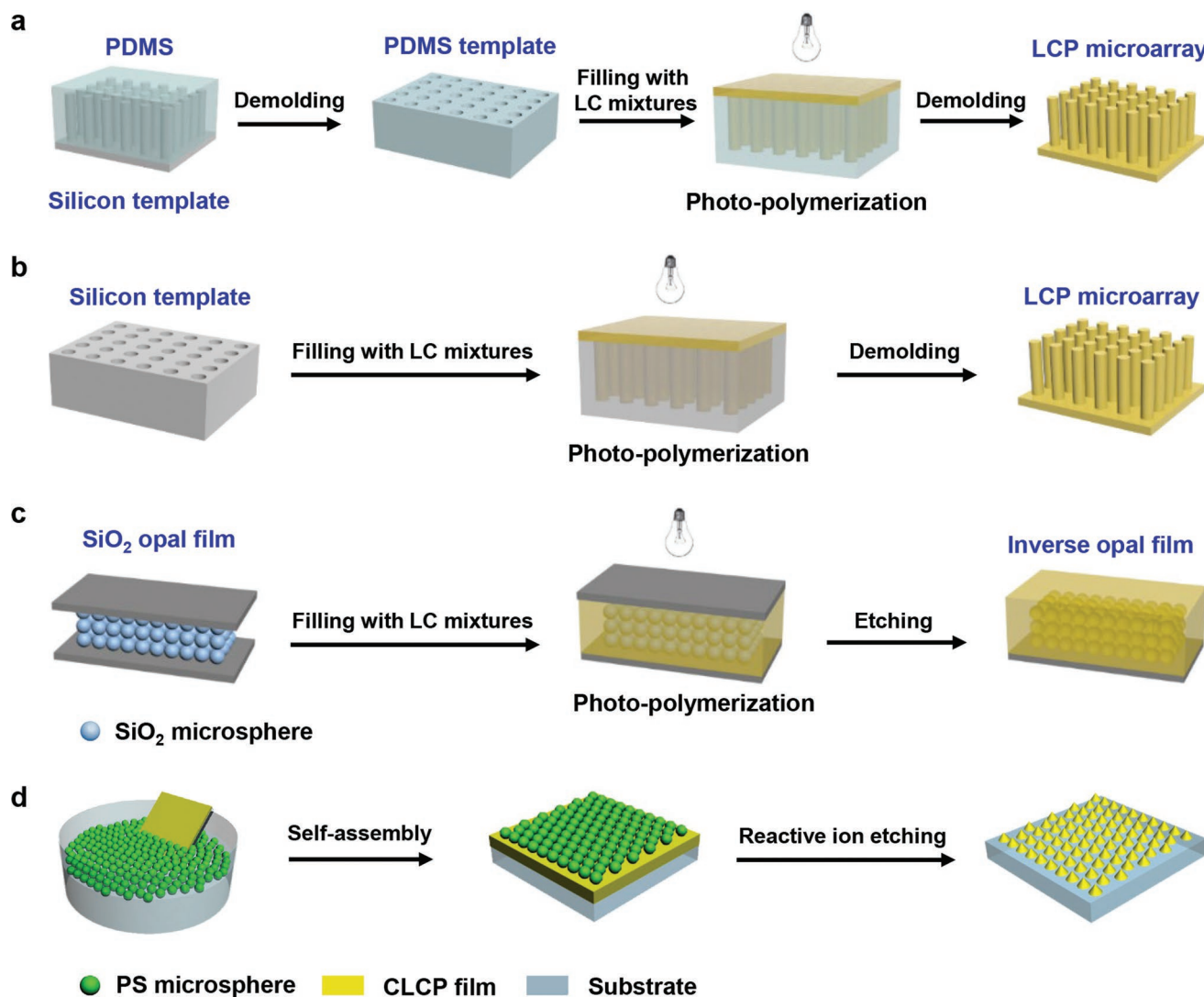


Figure 14. a) Schematic illustration of the microarrayed azobenzene LCP film prepared by PDMS-soft-template-based secondary replication. Reproduced with permission.^[152] Copyright 2012, The Royal Society of Chemistry. b) The fabrication process of the 2D CLCP microarray. Reproduced with permission.^[153] Copyright 2012, Wiley-VCH. c) The fabrication process of the CLCP inverse opal film. Reproduced with permission.^[154] Copyright 2014, The Royal Society of Chemistry. d) Submicrocone arrayed CLCP film is obtained by two steps: First, polystyrene (PS) microspheres are self-assembled on the surface of the cleaned CLCP film to form hcp 2D PS colloidal crystals monolayer via the modified interface method. Then, CLCP submicrocone arrays are obtained by a short time reactive ion etching using 2D PS colloidal crystals as masks. Reproduced with permission.^[155] Copyright 2015, American Chemical Society.

the submicron scale by using the replica molding technique. They employed a silicon template to prepare photoresponsive CLCP micropillar arrays with the mean diameter around 0.6 μm (Figure 14b).^[153] The reflection spectra of the microarray showed switchable behavior when irradiated with UV-vis light alternately. Using CLCPs as inverse opal materials, they further developed the dual-responsive tunable photonic crystals (Figure 14c).^[154] In this work, the light/thermal-responsive inverse opal films were first prepared by infiltrating the ordered assembly of SiO₂ spheres with a precursor capable of solidification, and followed by removing the SiO₂ template. Compared with aforementioned 2D photonic crystal, inverse opal films showed high reflection intensity under alternating irradiation with UV and visible light.

5.2.4. Colloidal Lithography

In addition to replica molding technique, the colloidal lithography method has been commonly used in recent years to prepare microstructural surfaces. This technique presents the advantages of time-saving and fine regulation of structural parameters such as shapes and dimensions. Applying this approach, Yu and co-workers fabricated a submicropillar arrayed CLCP film and a submicrocone arrayed CLCP film (Figure 14d) with different wettability due to the controllable surface topography by modulating different types of etching masks.^[155] It is envisioned that such a colloidal lithography method, in combination with CLCPs, can be implemented to produce submicron-scale actuators with a rich variety of

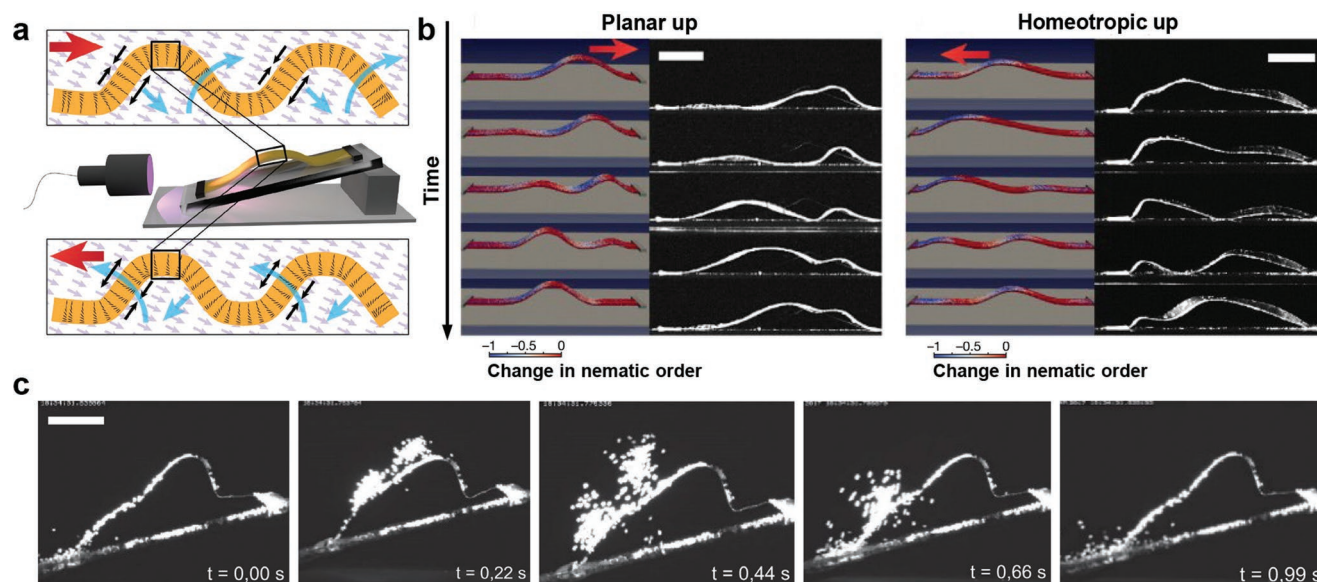


Figure 15. a) Schematic illustration of the experimental setup, showing a polymeric film which is constrained at both extremities under an oblique-incidence light source. The blue arrows show the way the film deforms while the red ones indicate the propagation direction of the wave. b) Comparison of simulation (left) and experimental data (right) for planar-up and homeotropic-up configurations. The arrows indicate the propagation direction of the wave. The scale bar represents the magnitude of the scalar order parameter, S (color scale: blue, low; red, high). Incident light: 10° from the left; $L = 22$ mm; scale bars: 5 mm; film size: 23 mm \times 4 mm \times 20 μ m. c) Photo-actuated wave motion ejects sand from the surface of the film via a snap-through release of energy, demonstrating the mechanism for a self-cleaning surface. Reproduced with permission.^[35] Copyright 2017, Springer Nature.

morphologies by regulating the etching masks throughout the fabrication process.

6. Application Prospects

6.1. Energy Harvesting

Laser-driven oscillations at high frequency and large amplitude have been generated using cantilevers made from CLCP films.^[22,24,156] These oscillations were induced by the *trans*–*cis*–*trans* reorientation of azobenzene groups. In 2010, Bunning and co-workers demonstrated fast and large oscillation movements with high frequency up to 270 Hz. Although the spontaneous movement of polymers upon exposure to external stimuli has been studied previously, the use of high-energy UV light potentially damages the material itself. The oscillation of azobenzene-containing CLCP cantilevers driven by sunlight opens up a new possibility in energy harvesting field.

Furthermore, Schenning and co-workers reported a self-oscillating sun and dual visible light–responsive soft actuator using an *ortho*-fluoroazobenzene (F-azo) as the photoisomerizable molecule.^[25] F-azos are photo-switchable moieties that are responsive to visible light. The *trans*–*cis* and *cis*–*trans* isomerizations of F-azo occur upon irradiation with green and blue light, respectively. When exposed to nonconcentrated sunlight in air, the continuous *trans* \leftrightarrow *cis* isomerizations of azobenzenes and the corresponding molecular motion caused the chaotic oscillatory motion of the splay-oriented CLCP film. This continuous motion obtained also allows for harvesting and conversion of solar energy. Moreover, the photogenerated shapes have a long lifetime since the *cis* isomer of the F-azo has a half-life up to years in solution.

6.2. Self-Cleaning Surfaces

Smart surfaces have already been developed for versatile applications such as self-healing,^[157] self-cleaning,^[25,35,158] etc. For instance, the water resources in the desert are extremely scarce, thus the self-cleaning of solar cell surfaces in the desert appears to be quite important. Continuous motion is needed for a smooth removal of particles from the surface. Broer et al. reported a novel CLCP device, which was capable of generating continuous, directional millimeter-scale mechanical waves fueled by a fixed light source (Figure 15).^[35] They developed an azobenzene derivative with push–pull groups. The delocalization of the electronic density of this azobenzene results in the fast thermal relaxation of CLCPs (i.e., *cis*–*trans* isomerization without light irradiation). They incorporated this azobenzene derivative into CLCP films and controlled the alignment of LC molecules—they were homeotropic (perpendicular to the surface) at one face, but planar (parallel to the surface) at the other. By attaching both ends of CLCP films to a substrate and irradiating them with UV light continuously, the wave propagation and regeneration were realized by self-shadowing of films. The alternating cyclic variations of the areas exposed to and hidden from the UV irradiation generated travelling waves in the films. The authors further showed that sand placed on the side of the film at which the wave originated was continuously transported toward the opposite side, and even was thrown far from the film, if there was a sudden release of energy. This work realizes an unprecedented macroscopic mechanical wave deformation through ingenious molecular and device design strategies. It is anticipated that the generation of waves has potential applications in self-cleaning surfaces.

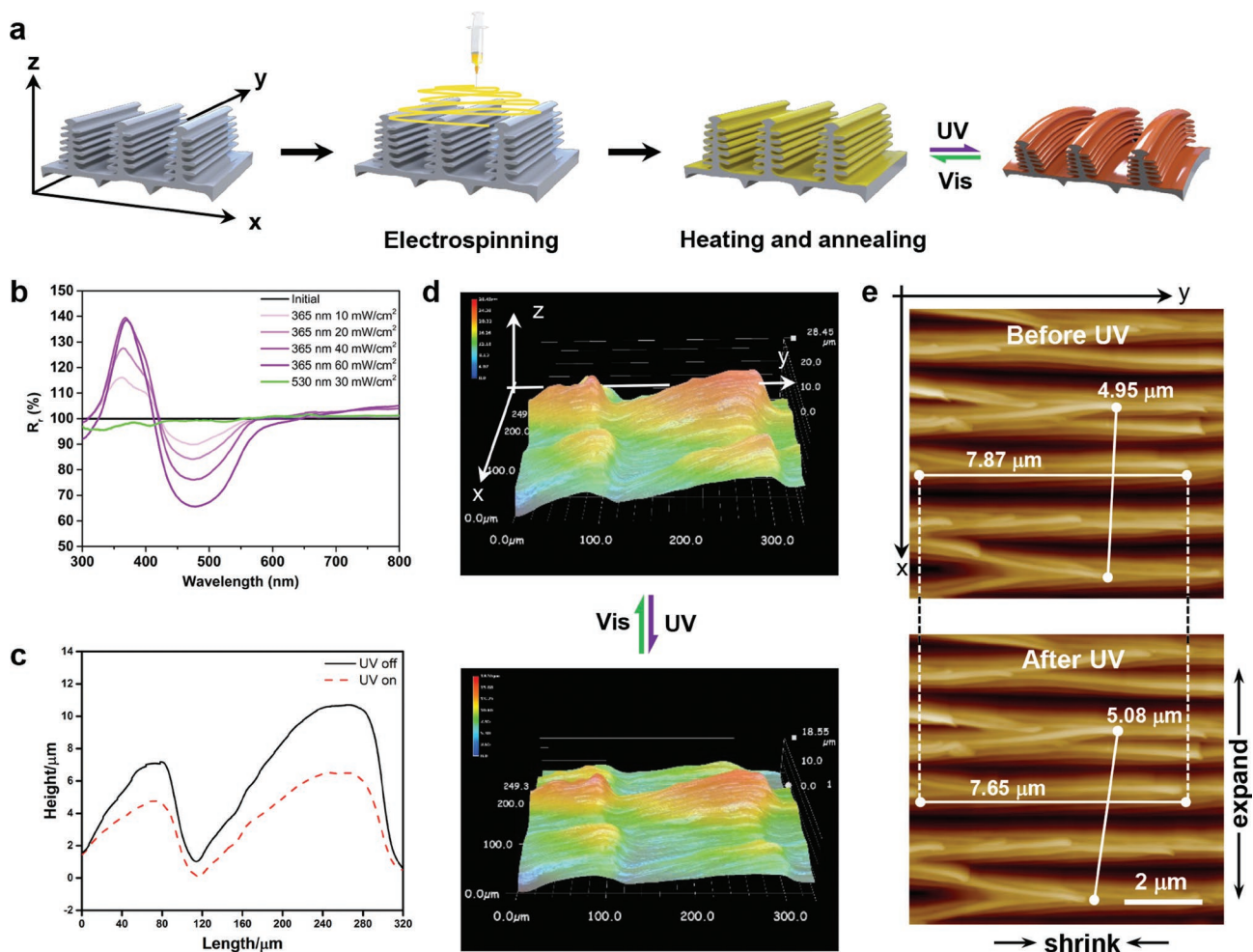


Figure 16. a) Schematic showing the fabrication of LLCPC-MBW and the reversible photo-induced deformation. b) Relative reflectance (R_r) of LLCPC-MBW shows the change ratio of reflection under different lights and intensities. c) Surface profiles and d) 3D reconstruction images of the scales on the LLCPC-MBW show the reversible deformation of the scales on LLCPC-MBW upon UV (365 nm, 10 mW cm⁻²) and visible light (white light from the microscope) irradiations. e) In situ AFM images of the microstructure on the LLCPC-MBW scales before and after UV irradiation. a–e) Reproduced with permission.^[159] Copyright 2018, Wiley-VCH.

6.3. Sensors

Photodeformable LCPs provide an efficient way for the design of light-controlled sensors. Recently, Yu et al. reported a new phototunable photonic crystal by coating an azobenzene-containing LLCPC as shown in Figure 12b onto *Morpho* butterfly wing (MBW) through electrospinning technique (Figure 16a).^[159] They observed the deformation of the hierarchical microstructures of the LLCPC-coated MBW (LLCPC-MBW) including scales, ridges, and lamellas for the first time (Figure 16b–d). Thanks to the excellent mechanical properties, especially the photodeformability of the LLCPC coating, this LLCPC-MBW presented an athermal and anisotropic deformation with a large shift of the reflection peak (≈ 70 nm) and a tunable reflection intensity (40%) upon the remote irradiation of low energy UV light (Figure 16e,f). Moreover, the deformation and the reflection intensity were controlled by the variation of the UV light intensity and were restored by visible light irradiation, showing potentials in light sensors.

In addition, the combination of photoresponsiveness with sensitivity to humidity of azobenzene-containing LCPs has been

reported to fabricate light/humidity sensors. Yu's group prepared a hydrophobic CLCP film capable of dual-responsive motion by utilizing UV light and humidity gradients.^[160] When exposed to UV light, the CLCP film bent along the LC alignment direction owing to a change in the molecular orientation triggered by the *trans*–*cis* isomerization of azobenzenes. In humid condition, water molecules formed weak hydrogen bonding interaction with the C=O and C–O–C groups in the hydrophobic CLCP, disrupting the alignment of mesogens. The disorder of alignment was further amplified by the cooperative motion of mesogens and translated into the expansion orthogonal to the bending direction induced by light. This work broadens the potential applications of the dual-responsive CLCP films in sensors.

6.4. Photo-Controlled Microfluidics

Creatures have the ability to transport liquids for survival by taking advantage of the Laplace effect. For example, long-billed birds complete feeding behaviors by changing shapes

of droplets through small-angle opening and closing of bills, and then propelling small amounts of liquids by the Laplace pressure difference.^[161] Enlightened by this phenomenon, Yu and co-workers proposed a new strategy to manipulate liquids by photo-induced asymmetric capillary force (**Figure 17a,b**).^[30] They first fabricated tubular microactuators (TMAs) by using a novel LLCP with enough mechanical robustness in the absence of chemical crosslinks. The photo-induced reorientation of azobenzene mesogens under 470 nm light triggered the geometric change of the TMA from cylindrical to conical shape. This cone-like geometry generated asymmetric

capillary force to propel liquids toward the light attenuated direction.

The TMAs were applicable to propel simple liquids spanning nonpolar to polar liquids, but also complex fluids used in the fields of biomedicine and chemical engineering, such as vegetable oil, serum albumin solution, cell culture medium, etc., which greatly enriched the types of light-controlled microliquids.^[162] The propelling speed of a liquid in the TMA reached up to 5.9 mm s^{-1} , and the moving distance reached to 57 mm, which were the highest records of liquid motion driven by photo-induced capillary force found so far. Without any

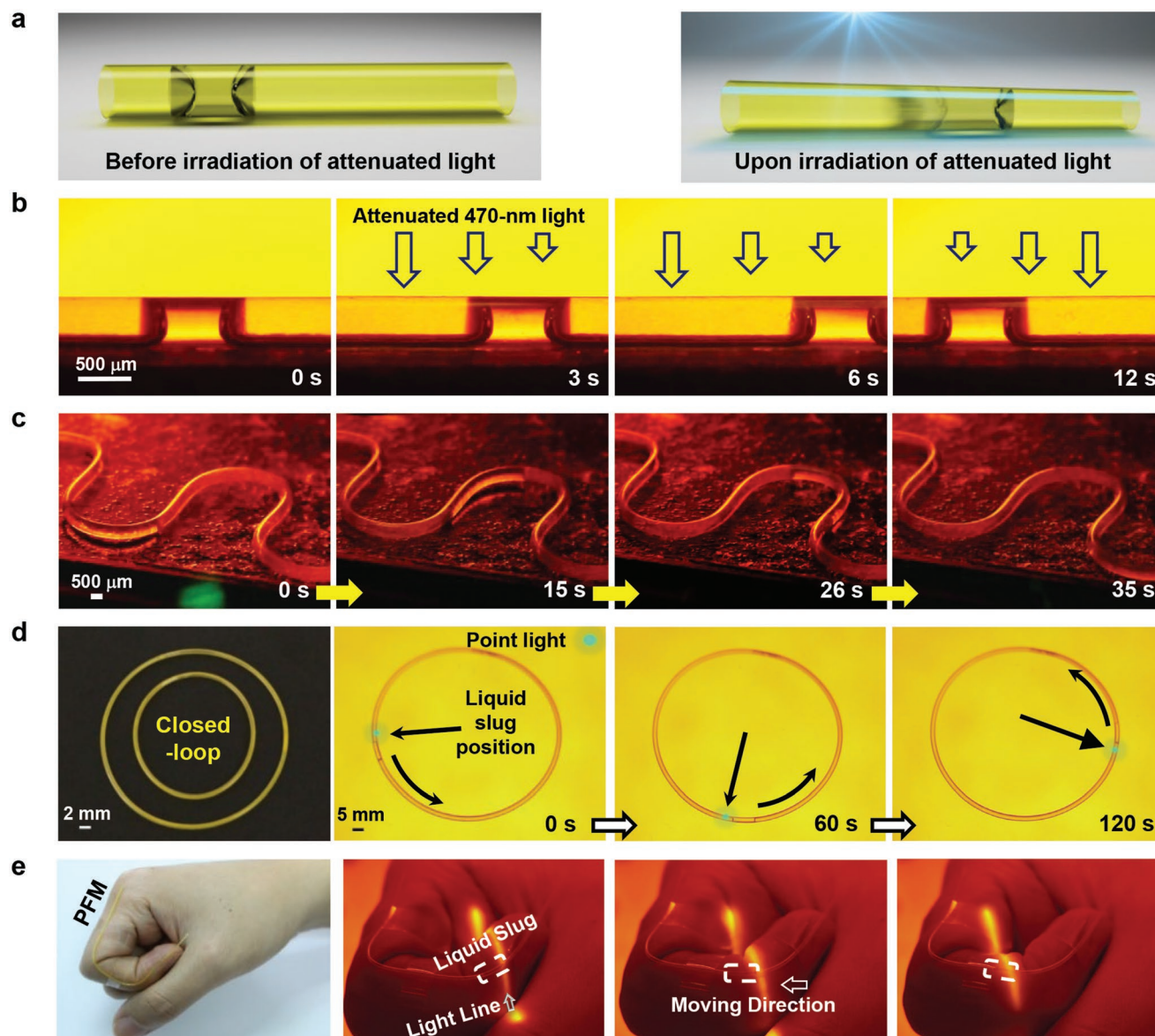


Figure 17. a) Schematics showing the motion of a slug of fully wetting liquid confined in a TMA driven by photodeformation. b) Lateral photographs of the light-induced motion of a silicone oil slug in a TMA fixed on a substrate that are taken through an optical filter to remove light with wavelengths below 530 nm. c) Lateral photographs showing light-driven motion of a silicone oil slug in a serpentine TMA. a–c) Reproduced with permission.^[30] Copyright 2016, Springer Nature. d) Photographs of the closed-loop actuator fabricated of PFMs by end-to-end connection. 3 mL isopropanol is preloaded into the reactor. The light spot with an intensity of 120 mW cm^{-2} is located at the end of the confined slug. e) Photo-controlled transport of an isopropanol slug in a PFM which is attached on the index finger upon the irradiation of 470 nm line light (80 mW cm^{-2}). d,e) Reproduced with permission.^[128] Copyright 2019, Wiley-VCH.

auxiliary devices, TMAs were also capable of propelling liquid on a horizontal “S”-shaped trajectory (Figure 17c). In addition, the liquid mixing, as well as the capture and movement of microspheres on the microscale was realized in the TMAs. These photodeformable TMAs are considered as excellent candidates for applications in the fields of micro-reactors, lab-on-chip, and micro-optomechanical systems.^[163]

Except for the single layer microtube, Yu et al. also developed a bilayer flexible microtube containing an outer flexible EVA supporting layer and an inner photodeformable LLCPLCP layer, which was capable of propelling various liquids by light toward the predetermined direction.^[128] The photo-induced reorientation of the azobenzene mesogens in the LLCPLCP layer triggered the geometric change of the bilayer microtube and generated the asymmetric capillary force. For example, the supporting EVA layer provided elasticity for tight connection between PFM themselves or other microtubes. A closed-loop microfluidic actuator was created with an airtight joint through the simple end-to-end connection of one PFM (Figure 17d). Upon irradiation of 470 nm light, the inner isopropanol slug was propelled counterclockwise in the closed-loop actuator, where the liquid motion was hard to be driven by the conventional syringe pumps. This reveals that the closed-looped PFM is ideal for implementing biological reactions and analysis as it prevents solvent evaporation and contamination from the external environment. Furthermore, an example of liquid motion on fingers was demonstrated to explore the potential application of the PFM in wearable systems (Figure 17e). Under the 470 nm light, the liquid slug was manipulated away from the fingertip in curved state. This feature was ascribed to the bilayer structure of the PFM, which was capable of being changed into arbitrary 3D shapes (trajectories) and preserved photodeformability to propel the inner liquids. It has been anticipated that these PFMs will find use in micro-electromechanical systems and lab-on-a-chip settings as the photo-controllable components and liquid manipulation tools.

7. Conclusion and Perspectives

In this review, we have summarized the progress made in the photodeformable LCPs over the past decades. The focus is placed on light as a trigger because it is clean, remote, tunable in intensity and wavelength, and nondestructive. Scientists have developed a wide variety of LCP actuators able to bend, twist, or oscillate in response to light. A breakthrough in the LCP field came with the development of bioinspired LCP actuators able to mimic the behaviors and functions of organisms in a dynamic, adjustable, and reversible way.

The diversity of deformation modes of LCPs is closely related to the innovative materials. The acrylate and siloxane CLCPs were developed in the beginning, then a series of newly synthesized photodeformable LCPs containing special chemical structures such as post-crosslinkable moieties, dynamic covalent bonding, and linear structure without chemical crosslinks flourished. Urged by the material innovations, the processing performance of photodeformable LCPs has made monumental leaps forward, from the original processing of films and fibers to the fabrication of complex 3D actuators. Thus, developing

LCPs with improved processability is an important direction in the future.

Microstructured LCP actuators that respond to light source often stimulate the development of new applications, such as autonomous microrobots, smart surfaces, sensing particles, etc. A series of new preparation techniques such as inkjet printing, microfluidics, template replication, and two-photon direct writing have emerged over the past 10 years, resulting in the dimension of actuators ranging from micron-level to the nanometer level.^[15–17,65] These novel preparation techniques broaden the application of photodeformable LCPs in microsystems, since it is extremely difficult to realize the response behaviors in micro- or nanoscale with traditional materials and methods. The fabrication of small-scale photodeformable LCP actuators ought to be one of the core subjects in future research, which requires not only the guidance from new concepts and theories, but also the assistance of innovative materials and technologies.

The development of processing techniques also provides a new opportunity of designing programmable LCPs, which have garnered great interests in developing smart robotic devices.^[164] The programming process may involve many aspects, such as the spatially modulation of the orientation of LCs and the special design of the geometry and composition. We even envision that the programmable control of light source allows for the programmable deformations of LCP actuators. Using the programming process to achieve complex and diverse shape-changing behaviors in LCP actuators will be a hot topic in the future.

Regarding the development of functions, the display functions of LCPs will not be limited to the changes in deformation modes. Instead, full advantages should be taken of the abundant deformation performances of LCPs to realize various functions in practical applications, such as micro-mechanical operation, biochemical testing, lab-on-chip, etc. The realization of functions will be achieved mainly by means of bionics to learn how animals or plants manipulate and convert energy, and take inspirations from nature to further design and develop novel functional devices.

Acknowledgements

This work was financially supported by the National Natural Science Foundation of China (21734003) and Innovation Program of Shanghai Municipal Education Commission (2017-01-07-00-07-E00027).

Conflict of Interest

The authors declare no conflict of interest.

Keywords

azobenzenes, bionic functions, liquid crystal polymers, photo-induced deformations, soft actuators

Received: July 3, 2019
Revised: August 10, 2019
Published online: October 9, 2019

- [1] T. Ikeda, J. Mamiya, Y. L. Yu, *Angew. Chem., Int. Ed.* **2007**, *46*, 506.
- [2] C. J. Barrett, J.-I. Mamiya, K. G. Yager, T. Ikeda, *Soft Matter* **2007**, *3*, 1249.
- [3] J. Wei, Y. L. Yu, *Soft Matter* **2012**, *8*, 8050.
- [4] H. R. Jiang, C. S. Li, X. Z. Huang, *Nanoscale* **2013**, *5*, 5225.
- [5] T. Ube, T. Ikeda, *Angew. Chem., Int. Ed.* **2014**, *53*, 10290.
- [6] X. Qing, L. Qin, W. Gu, Y. L. Yu, *Liq. Cryst.* **2016**, *43*, 2114.
- [7] H. K. Bisoyi, L. Quan, *Chem. Rev.* **2016**, *116*, 15089.
- [8] X. Qing, J.-A. Lv, Y. L. Yu, *Acta Polym. Sin.* **2017**, *11*, 1679.
- [9] W. Gu, X. Qing, J. Wei, Y. L. Yu, *Chin. Sci. Bull.* **2016**, *61*, 2102.
- [10] E. Pantuso, G. D. Filpo, F. P. Nicoletta, *Adv. Opt. Mater.* **2019**, *7*, 1900252.
- [11] L. Matějka, K. Dušek, M. Ilavský, *Polym. Bull.* **1979**, *1*, 659.
- [12] L. Matějka, M. Ilavský, K. Dušek, O. Wichterle, *Polymer* **1981**, *22*, 1511.
- [13] L. Matějka, K. Dušek, *Die Makromol. Chem.* **1981**, *182*, 3223.
- [14] Q. M. Zhang, M. J. Serpe, *ChemPhysChem* **2017**, *18*, 1451.
- [15] T. J. White, *J. Polym. Sci., Part B: Polym. Phys.* **2018**, *56*, 695.
- [16] A. Rešetič, J. Milavec, B. Zupančič, V. Domenici, B. Zalar, *Nat. Commun.* **2016**, *7*, 13140.
- [17] H. Finkelmann, E. Nishikawa, G. G. Pereira, M. Warner, *Phys. Rev. Lett.* **2001**, *87*, 015501.
- [18] T. Ikeda, M. Nakano, Y. L. Yu, O. Tsutsumi, A. Kanazawa, *Adv. Mater.* **2003**, *15*, 201.
- [19] Y. L. Yu, M. Nakano, T. Ikeda, *Nature* **2003**, *425*, 145.
- [20] C. L. van Oosten, C. W. Bastiaansen, D. J. Broer, *Nat. Mater.* **2009**, *8*, 677.
- [21] S. Iamsaard, S. J. Asshoff, B. Matt, T. Kudernac, J. J. L. M. Cornelissen, S. P. Fletcher, N. Katsonis, *Nat. Chem.* **2014**, *6*, 229.
- [22] K. M. Lee, M. L. Smith, H. Koerner, N. Tabiryan, R. A. Vaia, T. J. Bunning, T. J. White, *Adv. Funct. Mater.* **2011**, *21*, 2913.
- [23] K. M. Lee, T. J. Bunning, T. J. White, *Adv. Mater.* **2012**, *24*, 2839.
- [24] T. J. White, N. V. Tabiryan, S. V. Serak, U. A. Hrozhyk, V. P. Tondiglia, H. Koerner, R. A. Vaia, T. J. Bunning, *Soft Matter* **2008**, *4*, 1796.
- [25] K. Kumar, C. Knie, D. Bleger, M. A. Peletier, H. Friedrich, S. Hecht, D. J. Broer, M. G. Debije, A. P. Schenning, *Nat. Commun.* **2016**, *7*, 11975.
- [26] C. Ohm, M. Brehmer, R. Zentel, *Adv. Mater.* **2010**, *22*, 3366.
- [27] H. Yang, A. Buguin, J. M. Taulemesse, K. Kaneko, S. Mery, A. Bergeret, P. Keller, *J. Am. Chem. Soc.* **2009**, *131*, 15000.
- [28] H. Zeng, P. Wasylczyk, C. Parmeggiani, D. Martella, M. Burresti, D. S. Wiersma, *Adv. Mater.* **2015**, *27*, 3883.
- [29] E. K. Fleischmann, H. L. Liang, N. Kapernaum, F. Giesselmann, J. Lagerwall, R. Zentel, *Nat. Commun.* **2012**, *3*, 1178.
- [30] J.-A. Lv, Y. Y. Liu, J. Wei, E. Q. Chen, L. Qin, Y. L. Yu, *Nature* **2016**, *537*, 179.
- [31] M. Yamada, M. Kondo, R. Miyasato, Y. Naka, J. Mamiya, M. Kinoshita, A. Shishido, Y. L. Yu, C. J. Barrett, T. Ikeda, *J. Mater. Chem.* **2009**, *19*, 60.
- [32] S. J. Asshoff, F. Lancia, S. Iamsaard, B. Matt, T. Kudernac, S. P. Fletcher, N. Katsonis, *Angew. Chem., Int. Ed.* **2017**, *56*, 3261.
- [33] G. Stoychev, A. Kirillova, L. Ionov, *Adv. Opt. Mater.* **2019**, *7*, 1900067.
- [34] T. Ikeda, T. Ube, *Mater. Today* **2011**, *14*, 480.
- [35] A. H. Gelebart, D. Jan Mulder, M. Varga, A. Konya, G. Vantomme, E. W. Meijer, R. L. B. Selinger, D. J. Broer, *Nature* **2017**, *546*, 632.
- [36] X. Lu, H. Zhang, G. Fei, B. Yu, X. Tong, H. S. Xia, Y. Zhao, *Adv. Mater.* **2018**, *30*, 1706597.
- [37] L. Liu, M. H. Liu, L. L. Deng, B. P. Lin, H. Yang, *J. Am. Chem. Soc.* **2017**, *139*, 11333.
- [38] F. J. Ge, R. Yang, X. Tong, F. Camerel, Y. Zhao, *Angew. Chem., Int. Ed.* **2018**, *57*, 11758.
- [39] A. H. Gelebart, G. Vantomme, E. W. Meijer, D. J. Broer, *Adv. Mater.* **2017**, *29*, 1606712.
- [40] L. L. Dong, Y. Zhao, *Mater. Chem. Front.* **2018**, *2*, 1932.
- [41] H. K. Bisoyi, A. M. Urbas, Q. Li, *Adv. Opt. Mater.* **2018**, *6*, 1800458.
- [42] Y. Y. Zhang, J. X. Wang, T. Ikeda, L. Jiang, *J. Mater. Chem. C* **2019**, *7*, 3413.
- [43] H. Koerner, T. J. White, N. V. Tabiryan, T. J. Bunning, R. A. Vaia, *Mater. Today* **2008**, *11*, 34.
- [44] G. Vantomme, A. H. Gelebart, D. J. Broer, E. W. Meijer, *Tetrahedron* **2017**, *73*, 4963.
- [45] J.-I. Mamiya, A. Kuriyama, N. Yokota, M. Yamada, T. Ikeda, *Chem. - Eur. J.* **2015**, *21*, 3174.
- [46] Y. L. Yu, T. Ikeda, *Angew. Chem., Int. Ed.* **2006**, *45*, 5416.
- [47] Q. Yu, B. Aguila, J. Gao, P. X. Xu, Q. Z. Chen, J. Yan, D. Xing, Y. Chen, P. Cheng, Z. J. Zhang, S. Q. Ma, *Chem. - Eur. J.* **2019**, *25*, 5611.
- [48] A. Priimagi, C. J. Barrett, A. Shishido, *J. Mater. Chem. C* **2014**, *2*, 7155.
- [49] H. Zeng, P. Wasylczyk, D. S. Wiersma, A. Priimagi, *Adv. Mater.* **2018**, *30*, 1703554.
- [50] T. J. White, D. J. Broer, *Nat. Mater.* **2015**, *14*, 1087.
- [51] T. Ikeda, O. Tsutsumi, *Science* **1995**, *268*, 1873.
- [52] F. Weigert, *Verh. Dtsch. Phys. Ges.* **1919**, *21*, 479.
- [53] Y. L. Yu, T. Ikeda, Q. J. Zhang, *Adv. Mater.* **1999**, *11*, 300.
- [54] P. Weis, W. Tian, S. Wu, *Chem. - Eur. J.* **2018**, *24*, 6494.
- [55] P. G. deGennes, *C. R. Hebd. Séances Acad. Sci., Ser. B* **1975**, *281*, 101.
- [56] P. G. deGennes, M. Hebert, R. Kant, *Macromol. Symp.* **1997**, *113*, 39.
- [57] M. H. Li, P. Keller, B. Li, X. G. Wang, M. Brunet, *Adv. Mater.* **2003**, *15*, 569.
- [58] L. T. de Haan, A. P. H. J. Schenning, D. J. Broer, *Polymer* **2014**, *55*, 5885.
- [59] H. R. Trebin, *Adv. Phys.* **1982**, *31*, 195.
- [60] C. D. Modes, K. Bhattacharya, M. Warner, *Phys. Rev. E* **2010**, *81*, 060701.
- [61] C. D. Modes, K. Bhattacharya, M. Warner, *Proc. R. Soc. A* **2011**, *467*, 1121.
- [62] L. T. de Haan, C. Sanchez-Somolinos, C. M. Bastiaansen, A. P. Schenning, D. J. Broer, *Angew. Chem., Int. Ed.* **2012**, *51*, 12469.
- [63] M. E. McConney, A. Martinez, V. P. Tondiglia, K. M. Lee, D. Langley, I. I. Smalyukh, T. J. White, *Adv. Mater.* **2013**, *25*, 5880.
- [64] S. K. Ahn, T. H. Ware, K. M. Lee, V. P. Tondiglia, T. J. White, *Adv. Funct. Mater.* **2016**, *26*, 5819.
- [65] D. Q. Liu, D. J. Broer, *Responsive Polymer Surfaces: Dynamics in Surface Topography*, Wiley, Hoboken, NJ **2017**.
- [66] D. Q. Liu, *Liq. Cryst.* **2016**, *43*, 2136.
- [67] D. Q. Liu, C. W. M. Bastiaansen, J. M. J. den Toonder, D. J. Broer, *Angew. Chem., Int. Ed.* **2012**, *51*, 892.
- [68] D. Q. Liu, C. W. M. Bastiaansen, J. M. J. den Toonder, D. J. Broer, *Macromolecules* **2012**, *45*, 8005.
- [69] D. Q. Liu, D. J. Broer, *Angew. Chem., Int. Ed.* **2014**, *53*, 4542.
- [70] D. Q. Liu, L. Liu, P. R. Onck, D. J. Broer, *Proc. Natl. Acad. Sci. U. S. A.* **2015**, *112*, 3880.
- [71] D. Q. Liu, D. J. Broer, *Nat. Commun.* **2015**, *6*, 8334.
- [72] Y. L. Yu, M. Nakano, A. Shishido, T. Shiono, T. Ikeda, *Chem. Mater.* **2004**, *16*, 1637.
- [73] M. Kondo, R. Miyasato, Y. Naka, J.-I. Mamiya, M. Kinoshita, Y. L. Yu, C. J. Barrett, T. Ikeda, *Liq. Cryst.* **2009**, *36*, 1289.
- [74] A. Shimamura, A. Priimagi, J.-I. Mamiya, T. Ikeda, Y. L. Yu, C. J. Barrett, A. Shishido, *ACS Appl. Mater. Interfaces* **2011**, *3*, 4190.
- [75] W. K. Lee, K. N. Kim, M. F. Achard, J. I. Jin, *J. Mater. Chem.* **2006**, *16*, 2289.
- [76] Y. Y. Zhang, J. X. Xu, F. T. Cheng, R. Y. Yin, C. C. Yen, Y. L. Yu, *J. Mater. Chem.* **2010**, *20*, 7123.
- [77] A. Sánchez-Ferrer, A. Merekalov, H. Finkelmann, *Macromol. Rapid Commun.* **2011**, *32*, 671.
- [78] A. Priimagi, A. Shimamura, M. Kondo, T. Hiraoka, S. Kubo, J.-I. Mamiya, M. Kinoshita, T. Ikeda, A. Shishido, *ACS Macro Lett.* **2012**, *1*, 96.

- [79] M. Kondo, M. Sugimoto, M. Yamada, Y. Naka, J. Mamiya, M. Kinoshita, A. Shishido, Y. L. Yu, T. Ikeda, *J. Mater. Chem.* **2010**, *20*, 117.
- [80] M. Kondo, Y. L. Yu, T. Ikeda, *Angew. Chem., Int. Ed.* **2006**, *45*, 1378.
- [81] R. Y. Yin, W. X. Xu, M. Kondo, C. C. Yen, J.-I. Mamiya, T. Ikeda, Y. L. Yu, *J. Mater. Chem.* **2009**, *19*, 3141.
- [82] F. T. Cheng, Y. Y. Zhang, R. Y. Yin, Y. L. Yu, *J. Mater. Chem.* **2010**, *20*, 4888.
- [83] W. Wu, L. M. Yao, T. S. Yang, R. Y. Yin, F. Y. Li, Y. L. Yu, *J. Am. Chem. Soc.* **2011**, *133*, 15810.
- [84] Z. Jiang, M. Xu, F. Y. Li, Y. L. Yu, *J. Am. Chem. Soc.* **2013**, *135*, 16446.
- [85] Z. J. Wang, K. Li, Q. G. He, S. Q. Cai, *Adv. Mater.* **2019**, *31*, 1806849.
- [86] A. H. Gelebart, D. Q. Liu, D. J. Mulder, K. H. J. Leunissen, J. van Gerven, A. P. H. J. Schenning, D. J. Broer, *Adv. Funct. Mater.* **2018**, *28*, 1705942.
- [87] T. Ube, T. Ikeda, *Adv. Opt. Mater.* **2019**, *7*, 1900380.
- [88] M. Yamada, M. Kondo, J. Mamiya, Y. Yu, M. Kinoshita, C. J. Barrett, T. Ikeda, *Angew. Chem., Int. Ed.* **2008**, *47*, 4986.
- [89] F. T. Cheng, R. Y. Yin, Y. Y. Zhang, C. Yen, Y. L. Yu, *Soft Matter* **2010**, *6*, 3447.
- [90] M. Vilfan, A. Potocnik, B. Kavcic, N. Osterman, I. Poberaj, A. Vilfan, D. Babic, *Proc. Natl. Acad. Sci. U. S. A.* **2010**, *107*, 1844.
- [91] A. H. Gelebart, M. M. Bride, A. P. H. J. Schenning, C. N. Bowman, D. J. Broer, *Adv. Funct. Mater.* **2016**, *26*, 5322.
- [92] O. M. Wani, H. Zeng, A. Priimagi, *Nat. Commun.* **2017**, *8*, 15546.
- [93] O. M. Wani, R. Verpaalen, H. Zeng, A. Priimagi, A. P. H. J. Schenning, *Adv. Mater.* **2019**, *31*, 1805985.
- [94] Y. L. Yu, T. Maeda, J. Mamiya, T. Ikeda, *Angew. Chem.* **2007**, *119*, 899.
- [95] K. D. Harris, R. Cuyper, P. Scheibe, C. L. van Oosten, C. W. M. Bastiaansen, J. Lub, D. J. Broer, *J. Mater. Chem.* **2005**, *15*, 5043.
- [96] M. Wang, B. P. Lin, H. Yang, *Nat. Commun.* **2016**, *7*, 13981.
- [97] S. Iamsaard, E. Anger, S. J. Abhoff, A. Depauw, S. P. Fletcher, N. Katsonis, *Angew. Chem., Int. Ed.* **2016**, *55*, 9908.
- [98] S. Armon, E. Efrati, R. Kupferman, E. Sharon, *Science* **2011**, *333*, 1726.
- [99] J. J. Wie, M. R. Shankar, T. J. White, *Nat. Commun.* **2016**, *7*, 13260.
- [100] G. Han, J. Y. Nie, H. Q. Zhang, *Polym. Chem.* **2016**, *7*, 5088.
- [101] M. Petr, B.-A. Katzman, W. DiNatale, P. T. Hammond, *Macromolecules* **2013**, *46*, 2823.
- [102] Z. Q. Pei, Y. Yang, Q. M. Chen, E. M. Terentjev, Y. Wei, Y. Ji, *Nat. Mater.* **2014**, *13*, 36.
- [103] T. Yoshino, M. Kondo, J. Mamiya, M. Kinoshita, Y. L. Yu, T. Ikeda, *Adv. Mater.* **2010**, *22*, 1361.
- [104] Z. X. Cheng, S. D. Ma, Y. H. Zhang, S. Huang, Y. X. Chen, H. F. Yu, *Macromolecules* **2017**, *50*, 8317.
- [105] X. J. Li, R. B. Wen, Y. Zhang, L. R. Zhu, B. L. Zhang, H. Q. Zhang, *J. Mater. Chem.* **2009**, *19*, 236.
- [106] G. Han, H. T. Zhang, J. Chen, Q. Sun, Y. Y. Zhang, H. Q. Zhang, *New J. Chem.* **2015**, *39*, 1410.
- [107] L. J. Fang, G. Han, J. Y. Zhang, H. T. Zhang, H. Q. Zhang, *Eur. Polym. J.* **2015**, *69*, 592.
- [108] J.-A. Lv, W. Wang, W. Wu, Y. L. Yu, *J. Mater. Chem. C* **2015**, *3*, 6621.
- [109] Y. Y. Liu, W. Wu, J. Wei, Y. L. Yu, *ACS Appl. Mater. Interfaces* **2017**, *9*, 782.
- [110] X. L. Pang, B. Xu, X. Qing, J. Wei, Y. L. Yu, *Macromol. Rapid Commun.* **2018**, *39*, 1700237.
- [111] D. Montarnal, M. Capelot, F. Tournilhac, L. Leibler, *Science* **2011**, *334*, 965.
- [112] P. Chakma, D. Konkolewicz, *Angew. Chem., Int. Ed.* **2019**, *58*, 9682.
- [113] T. Ube, K. Kawasaki, T. Ikeda, *Adv. Mater.* **2016**, *28*, 8212.
- [114] Y. Z. Li, O. Rios, J. K. Keum, J. Chen, M. R. Kessler, *ACS Appl. Mater. Interfaces* **2016**, *8*, 15750.
- [115] Y. Yang, Z. Q. Pei, X. Q. Zhang, L. Tao, Y. Wei, Y. Ji, *Chem. Sci.* **2014**, *5*, 3486.
- [116] Y. Yang, Z. Q. Pei, Z. Li, Y. Wei, Y. Ji, *J. Am. Chem. Soc.* **2016**, *138*, 2118.
- [117] D. W. Hanzon, N. A. Traugutt, M. K. McBride, C. N. Bowman, C. M. Yakacki, K. Yu, *Soft Matter* **2018**, *14*, 951.
- [118] Y. Z. Li, Y. H. Zhang, O. Rios, J. K. Keum, M. R. Kessler, *RSC Adv.* **2017**, *7*, 37248.
- [119] M. K. McBride, A. M. Martinez, L. Cox, M. Alim, K. Childress, M. Beiswinger, M. Podgorski, B. T. Worrell, J. Killgore, C. N. Bowman, *Sci. Adv.* **2018**, *4*, eaat4634.
- [120] X. J. Qian, Q. M. Chen, Y. Yang, Y. S. Xu, Z. Li, Z. H. Wang, Y. H. Wu, Y. Wei, Y. Ji, *Adv. Mater.* **2018**, *30*, 1801103.
- [121] M. K. McBride, M. Hendriks, D. Q. Liu, B. T. Worrell, D. J. Broer, C. N. Bowman, *Adv. Mater.* **2017**, *29*, 1606509.
- [122] S. W. Ula, N. A. Traugutt, R. H. Volpe, R. R. Patel, K. Yu, C. M. Yakacki, *Liq. Cryst. Rev.* **2018**, *6*, 78.
- [123] Z. Q. Pei, Y. Yang, Q. M. Chen, Y. Wei, Y. Ji, *Adv. Mater.* **2016**, *28*, 156.
- [124] X. L. Lu, S. W. Guo, X. Tong, H. S. Xia, Y. Zhao, *Adv. Mater.* **2017**, *29*, 1606467.
- [125] Z. J. Wang, H. M. Tian, Q. G. He, S. Q. Cai, *ACS Appl. Mater. Interfaces* **2017**, *9*, 33119.
- [126] H. J. Choi, K.-U. Jeong, L.-C. Chien, M.-H. Lee, *J. Mater. Chem.* **2009**, *19*, 7124.
- [127] D.-Y. Kim, S.-A. Lee, H. J. Choi, L.-C. Chien, M.-H. Lee, K.-U. Jeong, *J. Mater. Chem. C* **2013**, *1*, 1375.
- [128] B. Xu, C. Y. Zhu, L. Qin, J. Wei, Y. L. Yu, *Small* **2019**, *15*, 1901847.
- [129] J.-I. Mamiya, *Photomechanical Energy Conversion with Crosslinked Liquid-Crystalline Polymers*, Springer, Tokyo, Japan **2014**.
- [130] J. Kupfer, H. Finkelmann, *Die Makromol. Chem., Rapid Commun.* **1991**, *12*, 717.
- [131] H. Finkelmann, G. Rehage, *Die Makromol. Chem., Rapid Commun.* **1980**, *1*, 31.
- [132] C.-K. Chang, C. M. W. Bastiaansen, D. J. Broer, H.-L. Kuo, *Adv. Funct. Mater.* **2012**, *22*, 2855.
- [133] J. E. Marshall, S. Gallagher, E. M. Terentjev, S. K. Smoukov, *J. Am. Chem. Soc.* **2014**, *136*, 474.
- [134] Y. L. Yu, M. Nakano, T. Ikeda, *Pure Appl. Chem.* **2004**, *76*, 1467.
- [135] X. M. Sun, W. Wang, L. B. Qiu, W. H. Guo, Y. L. Yu, H. S. Peng, *Angew. Chem., Int. Ed.* **2012**, *51*, 8520.
- [136] J. X. Xu, R. Y. Yin, Y. L. Yu, W. R. Wang, T. Ikeda, *Mol. Cryst. Liq. Cryst.* **2007**, *470*, 83.
- [137] J. Garcia-Amorós, H. Finkelmann, D. Velasco, *J. Mater. Chem.* **2011**, *21*, 1094.
- [138] A. Sánchez-Ferrer, H. Finkelmann, *Soft Matter* **2013**, *9*, 4621.
- [139] J. Garcia-Amorós, A. Piñol, H. Finkelmann, D. Velasco, *Org. Lett.* **2011**, *13*, 2282.
- [140] J. Garcia-Amorós, H. Finkelmann, D. Velasco, *Chem. - Eur. J.* **2011**, *17*, 6518.
- [141] J. Küpfer, H. Finkelmann, *Macromol. Chem. Phys.* **1994**, *195*, 1353.
- [142] A. R. Tajbakhsh, E. M. Terentjev, *Eur. Phys. J. E: Soft Matter Biol. Phys.* **2001**, *6*, 181.
- [143] A. Komp, H. Finkelmann, *Macromol. Rapid Commun.* **2007**, *28*, 55.
- [144] J. Cviklinski, A. R. Tajbakhsh, E. M. Terentjev, *Eur. Phys. J. E: Soft Matter Biol. Phys.* **2002**, *9*, 427.
- [145] R. Zentel, G. Reckert, *Die Makromol. Chem.* **1986**, *187*, 1915.
- [146] R. Zentel, M. Benalia, *Die Makromol. Chem.* **1987**, *188*, 665.
- [147] D. Iqbal, M. H. Samiullah, *Materials* **2013**, *6*, 116.
- [148] D. J. Broer, H. Finkelmann, K. Kondo, *Die Makromol. Chem.* **1988**, *189*, 185.
- [149] M. Singh, H. M. Haverinen, P. Dhagat, G. E. Jabbour, *Adv. Mater.* **2010**, *22*, 673.
- [150] H. Zeng, D. Martella, P. Wasylczyk, G. Cerretti, J. G. Lavocat, C. Ho, C. Parmeggiani, D. S. Wiersma, *Adv. Mater.* **2014**, *26*, 2319.

- [151] S. Palagi, A. G. Mark, S. Y. Reigh, K. Melde, T. Qiu, H. Zeng, C. Parmeggiani, D. Martella, A. Sanchez-Castillo, N. Kapernaum, F. Giesselmann, D. S. Wiersma, E. Lauga, P. Fischer, *Nat. Mater.* **2016**, *15*, 647.
- [152] C. Li, F. T. Cheng, J. Lv, Y. Zhao, M. J. Liu, L. Jiang, Y. L. Yu, *Soft Matter* **2012**, *8*, 3730.
- [153] Z. Yan, X. M. Ji, W. Wu, J. Wei, Y. L. Yu, *Macromol. Rapid Commun.* **2012**, *33*, 1362.
- [154] J. Q. Zhao, Y. Y. Liu, Y. L. Yu, *J. Mater. Chem. C* **2014**, *2*, 10262.
- [155] Y. Y. Zhan, J. Q. Zhao, W. D. Liu, B. Yang, J. Wei, Y. L. Yu, *ACS Appl. Mater. Interfaces* **2015**, *7*, 25522.
- [156] S. Serak, N. Tabiryan, R. Vergara, T. J. White, R. A. Vaia, T. J. Bunning, *Soft Matter* **2010**, *6*, 779.
- [157] H. W. Zhou, C. G. Xue, P. Weis, Y. Suzuki, S. L. Huang, K. Koynov, G. K. Auernhammer, R. Berger, H.-J. Butt, S. Wu, *Nat. Chem.* **2017**, *9*, 145.
- [158] W. Feng, D. J. Broer, D. Q. Liu, *Adv. Mater.* **2018**, *30*, 1704970.
- [159] X. Qing, Y. Y. Liu, J. Wei, R. Zheng, C. Y. Zhu, Y. L. Yu, *Adv. Opt. Mater.* **2019**, *7*, 1801494.
- [160] Y. Y. Liu, B. Xu, S. T. Sun, J. Wei, L. M. Wu, Y. L. Yu, *Adv. Mater.* **2017**, *29*, 1604792.
- [161] M. Prakash, D. Quere, J. W. Bush, *Science* **2008**, *320*, 931.
- [162] D. Baigl, *Lab Chip* **2012**, *12*, 3637.
- [163] Z. C. Dong, L. Jiang, *Sci. China Mater.* **2016**, *59*, 997.
- [164] L. Yu, H. Shahsavan, G. Rivers, C. Zhang, P. X. Si, B. X. Zhao, *Adv. Funct. Mater.* **2018**, *28*, 1802809.